

Review

# Advancement and Perspectives of Sulfite-Based Chemiluminescence, Its Mechanism, and Sensing

Syed Niaz Ali Shah <sup>1,\*</sup>, Eman Gul <sup>2</sup>, Faisal Hayat <sup>3</sup>, Ziaur Rehman <sup>3</sup> and Mashooq Khan <sup>4</sup>

<sup>1</sup> Innovation and Technology Transfer, King Fahd University of Petroleum and Minerals, Dhahran 31261, Saudi Arabia

<sup>2</sup> Institute of Chemical Sciences, University of Peshawar, Peshawar 25120, Pakistan

<sup>3</sup> Department of Chemistry, Quaid-I-Azam University, Islamabad 45320, Pakistan

<sup>4</sup> Qilu University of Technology (Shandong Academy of Sciences), Shandong Analysis and Test Center, Jinan 250014, China

\* Correspondence: niazalianalyst@gmail.com or syed.shah.3@kfupm.edu.sa

**Abstract:** This review sums up in detail the sulfite-based chemiluminescence (CL) systems and the impact of various enhancers such as metal ions and their complexes, solvents, nanomaterials (NMs), and carbon dots (CDs) on the CL system. Recent developments and strategies employed to enhance the sulfite-based CL systems are under lengthy discussion, especially in view of the emitting species and the reaction mechanism. The production of free radicals in the systems is thought to be critical for the improvement of the sulfite CL system due to their potential to degrade organic pollutants via advanced oxidation processes (AOPs). However, different chemicals can either favor or disfavor the formation of free radicals, ultimately having a positive or negative impact on CL response. Interestingly, these reagents can be easily differentiated by observing fluctuations in CL response with changes in concentration. We anticipate that an in-depth understanding of the mechanism of action of the sulfite CL system and the role of various enhancers on the efficiency of the system will be helpful in designing a highly selective and sensitive CL system for the detection of specific reagents. The development of improved sulfite CL systems, which use reagents that give a linear CL response with concentration, and their use in chemical, food and agricultural, forensic, pharmaceutical, clinical, agricultural, and environmental analysis is judiciously highlighted.

**Keywords:** sulfite; chemiluminescence; nanomaterials; review; carbon dots; quantum dots



**Citation:** Shah, S.N.A.; Gul, E.; Hayat, F.; Rehman, Z.; Khan, M. Advancement and Perspectives of Sulfite-Based Chemiluminescence, Its Mechanism, and Sensing.

*Chemosensors* **2023**, *11*, 212.

<https://doi.org/10.3390/chemosensors11040212>

[chemosensors11040212](https://doi.org/10.3390/chemosensors11040212)

Academic Editor: Luís C. Coelho

Received: 29 January 2023

Revised: 11 March 2023

Accepted: 20 March 2023

Published: 27 March 2023



**Copyright:** © 2023 by the authors. Licensee MDPI, Basel, Switzerland. This article is an open access article distributed under the terms and conditions of the Creative Commons Attribution (CC BY) license (<https://creativecommons.org/licenses/by/4.0/>).

## 1. Introduction

The production of electromagnetic radiation through a chemical reaction is called chemiluminescence (CL) [1,2]. In other words, in CL, an electrically stimulated chemical species emits light [3,4]. For example, reactants A and B, upon reaction, generate an electrically excited state, C\*, which emits radiations upon returning to its ground state (Figure 1) [4]. The intensity of CL is determined by the rate of the reaction as well as the ratio of the number of luminescent molecules to the number of molecules reacting (CL quantum efficiency). The majority of CL reactions emit minimal light and hence have a lower quantum efficiency. To address the issue, sensitizers, chemicals with a high fluorescence efficiency, are added to the CL reaction. An energy transfer from C\* to the sensitizer with a high fluorescence efficiency occurs, resulting in high emission [3]. The formed free radicals in CL produce unstable intermediates in the excited state, which either de-excite to the ground state accompanied by the emission of light or transfer energy to other luminophores. Normally, the energy produced by CL is more than 45 kcal/mol [5]. CL's advantages include high sensitivity, low cost, simplicity [5], low background noise [6], simple instrumentation, ease of automation [1], wide dynamic range and low detection limits. These factors influenced the interest in CL detection for flow injection analysis (FIA), high-performance liquid chromatography (HPLC), including miniature systems, and,

more recently, the rapidly expanding field of capillary electrophoresis [7] as well as in the microfluidic systems.

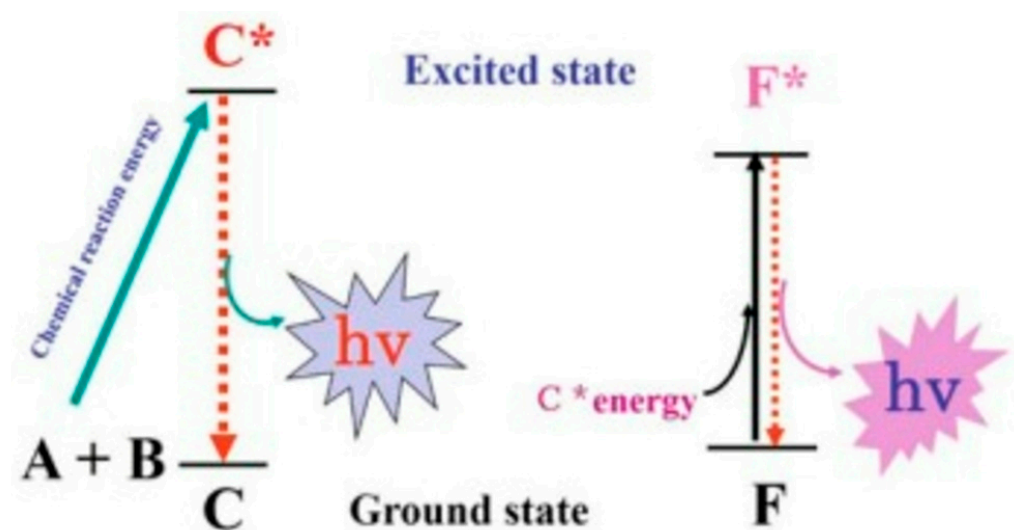


**Figure 1.** The basic principle of traditional and enhanced CL systems. Adapted with permission from [4], copyright 2022, Springer.

Among the reported CL systems, the sulfite-induced CL systems are the most fascinating ones. This review will focus on sulfite-induced CL systems and reagents that trigger their emission. The role of nanomaterials (NMs) in the enhancement of traditional CL systems will also be highlighted [8–10].

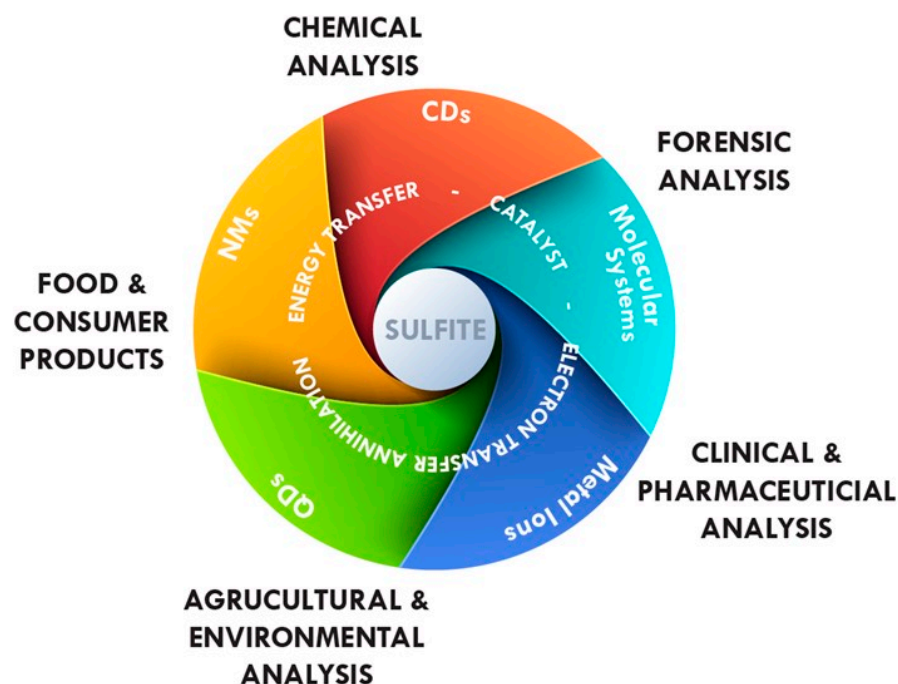
### 1.1. Sulfite

Sulfite refers to tetravalent sulfur-based substances such as sulfites ( $\text{SO}_3^{2-}$ ), sulfur dioxide ( $\text{SO}_2$ ), bisulfites ( $\text{HSO}_3^-$ ), and metabisulfites ( $\text{S}_2\text{O}_5^{2-}$ ) [11]. These compounds have antimicrobial, dehydrating, and preservative properties, making them useful in the food industry [5,12]. Sulfites are also used to bleach food starches and cherries, to avoid unwanted browning of fruits and vegetables, and are employed as a dough conditioner [13–15]. The significance of sulfites has also been established in the production of wood pulp in paper industries [12] and the remediation of aquatic pollution via advanced oxidation processes (AOPs) [16,17]. In addition to their advantages, sulfites also have some hazardous effects; for example, they are highly poisonous chemicals that are damaging to multiple human organs [18]. Furthermore, their presence in water can deplete oxygen to a harmful limit for aquatic life and can also be damaging to allergic individuals [12].

Sulfite oxidation has a long history of more than 50 years. The oxidation of sulfite was first proposed by a nucleophilic displacement of sulfite by hydrogen peroxide ( $\text{H}_2\text{O}_2$ ) [19,20]. Conversely, some researchers were in favor of the radical pathway for the  $\text{H}_2\text{O}_2$ -assisted oxidation of sulfite [21,22]. Notably, S (IV) species exist in different forms at different pHs in aqueous solutions: at a pH < 1.5 as  $\text{SO}_2 \cdot \text{H}_2\text{O}$ , at a pH 1.5–6.5 as  $\text{HSO}_3^-$  and at a pH > 6.5 as  $\text{SO}_3^{2-}$  [23]. So, pH plays a main role in the oxidation of S (IV) species [24]. As in sulfite, sulfur atoms have a lower valence than the expected maximum, so they are very popular in the industry and the environment and act as antioxidants in food and pharmaceuticals. In the wine industry, they are used as an inhibitor for yeast and bacteria [23]. The most interesting application of the oxidation of S (IV) species is in the desulfurization of industrial plume gases [25] and acid rain. Recently, it was also used for hydroxylation, epoxidation, and oxidative cleavage of DNA [26]. Natural oxidants oxidize S (IV) species in the atmosphere, producing revenue in gaseous and liquid forms such as clouds, fog, and raindrops. Among those natural oxidants,  $\text{H}_2\text{O}_2$  is considered the most potent in the aqueous phase [27].

### 1.2. Sulfite- $H_2O_2$ CL

The kinetics of the oxidation of aqueous sulfite by  $H_2O_2$  was studied by Frank et al. [27] and the mechanism by Shi et al. [28]. It was noted that sulfite oxidation was accompanied by CL emission [3]. The CL study of  $H_2O_2$  with different reagents, including sulfite, was reviewed in [29]. A weak CL is observed in the reaction of  $NaHSO_3$  with  $H_2O_2$  [30–32]. To overcome the lower CL efficiency problem of this traditional sulfite CL system, different enhancers, namely NMs and QDs, etc., were added [33]. The details of CL enhancers used in the sulfite system and their analytical application can be seen in Scheme 1. In this section, we discuss these enhancers in detail.



**Scheme 1.** Different enhancers are used to enhance the CL possession of sulfite-based systems. The various strategies to enhance the sulfite CL systems, the operating mechanisms and their applications in various fields are also described in the scheme.

### 1.3. CL Enhancers

Metal ions may increase or decrease the emission intensity of a particular CL system [34]. Surfactants are often used to enhance the CL intensity of different systems [3]. The microenvironment of the micelles protects the excited species from collisional quenching and other intermolecular processes which compete with the emission of light. The micelles solution not only protected the reactive species from water, preventing hydrolysis but also brought the reagents into close contact, considerably increasing CL quantum efficiency [35].

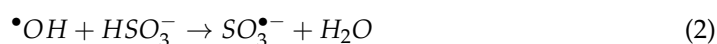
Due to their intriguing optical and electrical properties, chemical stability, and use in sensors, NMs have recently been a popular study topic in the field of catalysis and sensors [36]. Compared to the use of conventional dyes for CL enhancement, noble metal nanoclusters (NCs) have improved luminescence properties and have greater results in this area [37,38]. NM-based CL systems have emerged recently [39]. The role of NMs in an enhanced CL system is either as catalysts or energy acceptors or to undergo a reaction with the radicals to form the positively and negatively charged NMs. This finally results in the NMs in an excited state [40,41]. The method based on NPs' capacity to catalyze CL-reagent systems produces improved CL detection as a function of the NP species' redox catalytic capabilities, with activity correlated to their nature, composition, size, and shape [42]. In 2014, researchers from our group published a comprehensive review article on the role of quantum dots (QDs) in the enhancement of CL systems [8]. There are various other review articles on CL covering different areas [43,44].

Various efforts have been made to use CDs in the CL system [6,45,46]. The good solubility of CDs in water broadens their applications for reactions occurring in aqueous media [6,47–49]. In 2017, we reviewed in detail the role of CDs in the enhancement of CL systems [50].

## 2. Mechanism

The identification of free radicals, which can be determined by Electron paramagnetic resonance (EPR) spectroscopy [22,51], is critical for understanding this mechanism.

Sulfite, a potential reagent that can produce sulfate radicals during a catalytic reaction, has recently attracted more attention [52]. The  $\text{HSO}_3^-$  upon reaction with  $\text{H}_2\text{O}_2$  through a nucleophilic pathway forms peroxomonosulfurous acid [53] (Equation (1)), which then decomposes to  $\bullet\text{OH}$  and  $\text{SO}_3^{\bullet-}$  radicals [30,31], the main radicals in the  $\text{HSO}_3^-$  and  $\text{H}_2\text{O}_2$  CL systems [54]. In the propagation step,  $\bullet\text{OH}$  and  $\text{SO}_3^{\bullet-}$  convert other reactants to free radicals. For example, the  $\bullet\text{OH}$  radical reacts with  $\text{HSO}_3^-$  to form  $\text{SO}_3^{\bullet-}$  radicals (Equation (2)) [55], and in the subsequent step,  $\text{SO}_3^{\bullet-}$  radicals convert  $\text{H}_2\text{O}_2$  to a highly unstable superoxide radical ( $\text{O}_2^{\bullet-}$ ) (Equations (3) and (4)) [30,56].



In an acidic medium, sulfite ( $\text{SO}_3^{2-}$ ) forms the bisulfite ion  $\text{HSO}_3^-$  (Equation (5)).  $\text{HSO}_3^-$  can be oxidized by the oxidizing agent to form the  $\text{HSO}_3^{\bullet}$  radical (Equation (6)) [6].



$\text{HSO}_3^{\bullet}$  radicals combine to form  $\text{S}_2\text{O}_6^{2-}$  (Equation (7)), which decomposes from  $\text{SO}_2^*$  in the excited state (Equation (8)) [6].

In the sulfite CL systems, an unstable intermediate ( $\text{HO}_3\text{S-O-SO}_2\text{H}$ ) from hydrogen sulfite radicals is formed. The breakdown of this intermediate results in the formation of  $\text{SO}_2^*$  in the excited state, which emits in the range of 450–600 nm (Equation (9)) [6,43].  $^1\text{O}_2$  and  $\text{SO}_2^*$  are the main emitting species in the  $\text{NaHSO}_3\text{-H}_2\text{O}_2$  CL systems [54]. The emission quantum yields of these species are very low. Moreover, other emissive species with high emission quantum yield are usually added to get high CL emissions. In the case of highly fluorescent compounds, the transfer of energy from  $\text{SO}_2^*$  to efficient fluorophores can be assumed. Non-radiative dipole-dipole energy transfer from a CL donor to an appropriate acceptor is known as chemiluminescence resonance energy transfer (CRET); this is the highly operated mechanism in the presence of these fluorophores [1].

The mechanism of action for these surfactants and the micellar-enhanced CL systems is usually attributed to the stabilization of the radicals and emitting species [54]. Thus, micellar-involved CL systems result in high emissions compared to traditional molecular systems.

The singlet oxygen ( $^1\text{O}_2$ ), which is an electronically excited state, is mostly generated in many CL systems as the emissive species [57–60]. The different emissive species generated in the CL systems transfer their energy to the fluorescent compound with a high emission yield [61,62]. Due to the advent of certain nanomaterials as energy acceptors, CRET has advanced significantly [63,64].

### 3. Different Enhancers in Sulfite CL Systems

The different enhancers used so far for the enhancement of sulfite-based CL systems are summarized in Table 1 and are discussed under the following headings.

#### 3.1. CDs Enhanced Sulfite CL Systems

Amjadi et al. synthesized N and S-doped CDs and used them for the enhancement of the Mn-NaSO<sub>3</sub> CL system [65]. The reaction of Mn (IV) with the SO<sub>3</sub><sup>2-</sup> produced SO<sub>2</sub>\* in the excited state, and the transformation of SO<sub>2</sub>\* energy to the S, N-CDs resulted in an enhanced emission. The addition of oxytetracycline was found to linearly decrease the intensity of CL. The linear decrease in CL intensity vs. the concentration of oxytetracycline was observed to be in the range from 0.075 to 3.0 μmol/L with a 25 nmol/L limit of detection (LOD). The method was later on used for the determination of oxytetracycline in spiked milk and water samples.

Fan et al. used graphitic carbon nitride quantum dots (g-CNQDs) to enhance the CL intensity of a Ce (IV)-sulfite system [1]. The recombination of holes and electrons of the injected g-CNQDs was thought to enhance CL emission. Furthermore, the produced SO<sub>2</sub>\* from the interaction between Ce (IV) and sulfite transforms energy to the g-CNQDs. A resemblance of the given emission peak with the emission of the pristine g-CNQDs designated that the g-CNQDs is an emissive species (Figure 2a). The iodine quenches the CL intensity of this system owing to the reduction of Ce (IV) by the I<sup>-</sup>. The given CL system showed a linear response for I<sup>-</sup> concentration in the range from 3 × 10<sup>-7</sup> to 3 × 10<sup>-5</sup> mol/L. The forgoing method was found useful for the determination of I<sup>-</sup> in the urine samples.

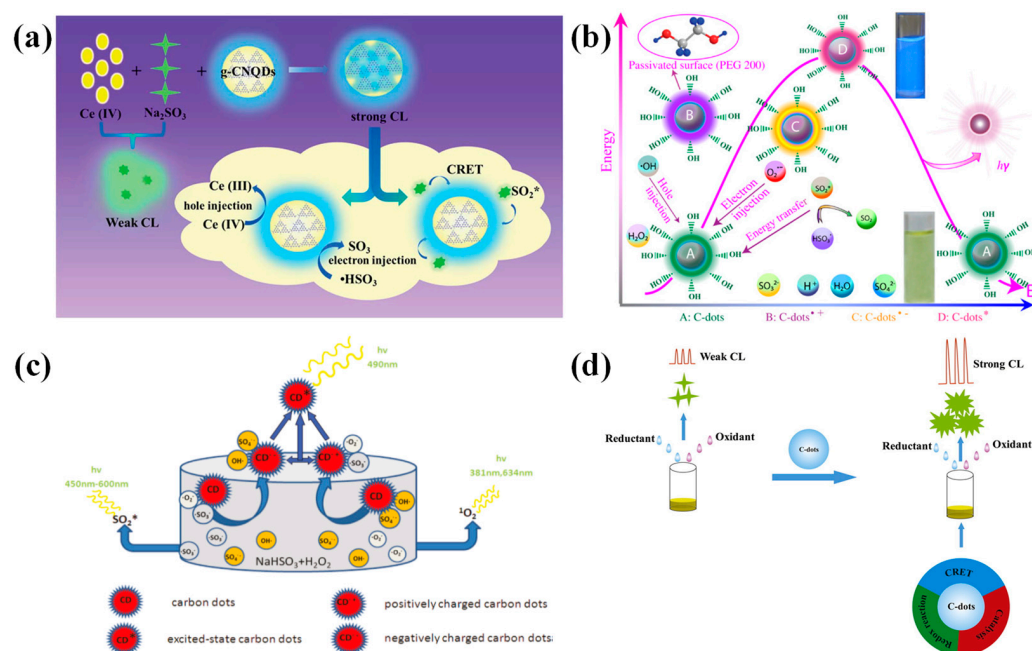


**Figure 2.** CDs enhanced sulfite CL systems. (a) The mechanism of emission from Ce (IV)-sulfite system in the presence of g-CNQDs. Reprinted with permission from [1], copyright 2016, Royal Society of Chemistry. (b) The reaction mechanism of CDs enhanced the peroxomonosulphate-sulfite system in an acidic medium. Reprinted with permission from [6], copyright 2012, Elsevier. (c) Reaction mechanism of the CL enhancement of NaHSO<sub>3</sub>-H<sub>2</sub>O<sub>2</sub> system by CDs. Adapted with permission from [31], copyright 2011, American Chemical Society. (d) The CL enhancement mechanism of CDs-sulfite system by bromate. Reprinted with permission from [50], copyright 2017, Elsevier.

Zhou et al. employed CDs to improve the CL intensity of peroxomonosulphate and the sulfite reaction in an acidic reaction [6]. The improvement was noted to stem from the energy transfer and electron transfer annihilation effect of CDs. The produced radicals were

found to react with the CDs to inject holes and electrons in the CDs. The electron-transfer annihilation process of the positively and negatively charged CDs results in excited CDs\*. On the other hand, the excited  $\text{SO}_2^*$  gave energy to the CDs. The final emission was from the CDs\* (Figure 2b). The CL of the aforementioned system was found to be inhibited by the aliphatic amines. The sensitized CL system was expended for the determination of aliphatic amines in water samples in a linear range from  $1 \times 10^{-5}$  to  $1 \times 10^{-9}$  mol/L. The CDs were used as enhancers for the bisulfite- $\text{H}_2\text{O}_2$  CL system [31]. The detailed mechanism of enhancement is elaborated in Figure 2c. The free radicals generated in the system were found responsible for generating holes in the valence band and electrons in the conduction band of the CDs. The electron annihilation effect was responsible for the generation of the excited states of the CDs, a reason for the enhanced CL. Li et al. used CDs and sulfite for the generation of CL signals [66]. The proposed CL method was used for the determination of bromate in water samples. A redox interaction between the CQDs, bromate, and sulfite in the acidic media caused the excitation of CDs due to electron and hole injection in the conduction and valence bands of CDs. Bromate is toxic to humans and other biotic components of the environment. The addition of bromate further enhanced the intensity of CL and was found to linearly increase with the increase in bromate concentrations. The given method was used for the determination of bromate in drinking water. The mechanism of the CDs-enhanced CL systems were recently reviewed in detail (Figure 2d) [50].

Zhang et al. reported mild CL by the traditional oxidation of bisulfite with hypochlorite, hydrogen peroxide, and permanganate [67]. They asserted that the inclusion of nitrogen-doped graphene quantum dots (N-GQD), nitrogen and sulfur-doped graphene quantum dots (N,S-GQD), or graphene quantum dots (GQD) considerably increases CL. An enhanced CL of the  $\text{NaHSO}_3$ - $\text{NaClO}$  system and the  $\text{NaHSO}_3$ - $\text{H}_2\text{O}_2$  system was observed in the neutral media, whereas for the  $\text{NaHSO}_3$ - $\text{KMnO}_4$  system in an acidic media. Additionally, the CL of the N,S-GQD- $\text{NaHSO}_3$ - $\text{NaClO}$  system was noticeably diminished by folic acid (FA; vitamin B9) and hence was declared a sensitive CL approach for the detection of FA in food samples.

### 3.2. NPs-QDs-Sulfite CL Systems

Nitrogen-doped graphene quantum dots (NGQDs) were used by Li et al. for the improvement of the CL intensity of the  $\text{KMnO}_4$ -sulfite system [68]. The pyridinic nitrogen on the surface of NGQDs converts the dissolved oxygen to  $\text{H}_2\text{O}_2$ . Furthermore, the phenolic groups on the surface of the NGQDs can chelate with the  $\text{Fe}^{3+}$  ions causing a reduction in CL intensity. A decrease in CL intensity was found to be linear, hence rendering the method worthwhile for the determination of  $\text{Fe}^{3+}$  ions in real water samples.

Liu et al. used an oleic acid-capped black phosphorus QDs (OA-BPQDs) enhanced  $\text{NaHSO}_3$  CL system [69]. The  $^1\text{O}_2$  and oxygen dipole species,  $(\text{O}_2)_2^*$ , used as emitting species, were generated from the  $\text{HSO}_3^-$  by the OA-BP QDs. The emitting species transfer their energy to the BP QDs capped with OA with an enhanced CL emission. The CL system was used for the determination of  $\text{SO}_3^{2-}$  in airborne fine particulate matter ( $\text{PM}_{2.5}$ ) (Figure 3a).

The low CL intensity of the traditional Ce (IV)-sulfite was due to the lower efficiency of  $\text{SO}_2^*$ . For the  $\text{Na}_2\text{SO}_3$ -Ce (IV) system, the weak CL was greatly enhanced by Yu et al. using modified Au NPs [70], which catalyzed the reaction resulting in higher production of  $\text{SO}_2^*$ , an excited state. The CL of the system was further enhanced when norfloxacin was introduced into it. The energy from  $\text{SO}_2^*$  flows to the norfloxacin on the surface of the Au NPs. The increase in CL intensity of the system was linear with the concentration of norfloxacin. The enhanced system was used for the determination of norfloxacin in human urine.

In another study, Yu et al. strongly enhanced the CL intensity of the weak CL Ce (IV)-sulfite system using silver nanocluster (Ag NCs) [37]. Ag NCs play a role in improving emissions by snatching energy from the  $\text{SO}_2^*$  intermediate. Cysteine was added to the system. The presence of Ag NCs enables the Ce (IV)-sulfite system to adsorb cysteine via

-SH bond interaction. The adsorbed cysteine hinders the energy transfer from  $\text{SO}_2^*$  to the Ag NCs, resulting in a diminished CL signal. They proposed that this system can be used for the detection of cysteine in the range from 5 nmol/L to 1  $\mu\text{mol/L}$  with 2.5 nmol/L LOD. In another attempt, Yu et al. observed that the inclusion of Ag NPs significantly improves the weak CL of the Ce (IV)- $\text{Na}_2\text{SO}_3$  redox system in the presence of  $\text{Tb}^{3+}$  and norfloxacin (NFLX) [71]. The Ag NPs speed up the process because of their electric activity. The intermediate  $\text{SO}_2^*$ , produced by the reaction of Ce (IV) with  $\text{Na}_2\text{SO}_3$ , contained energy that was transferred to  $\text{Tb}^{3+}$  via NFLX. NFLX flow injection determination was carried out using the proposed CL approach. The CL intensity, which rises linearly with NFLX concentration, was used to identify NFLX. NFLX in eyedrops was successfully determined using this approach.

$\text{Eu}^{3+}$ , Mohammad et al. were able to strengthen the weak CL signal produced by the reaction of Ce (IV) and  $\text{Na}_2\text{S}_2\text{O}_4$  [72]. The addition of naproxen (NAP) to this system dramatically boosted CL intensity. The energy of the intermediate state,  $\text{SO}_2^*$ , resulting from the redox reaction between Ce (IV) and  $\text{Na}_2\text{S}_2\text{O}_4$ , was transferred to  $\text{Eu}^{3+}$  with the assistance of NAP. Moreover, the catalytic activity of Ag NPs expedited this process. NAP determination is presented using a straightforward and exact CL method in combination with flow-injection technology. The assaying of NAP in commercially available NAP tablets was done using this approach.

Similarly, CdS QDs significantly improve the CL of the Ce (IV)- $\text{SO}_3^{2-}$  system [73]. The sensitizing effect was further enhanced by trace quantities of cetirizine. The suggested CL technique was used to determine cetirizine in pharmaceutical formulation. Likewise, Sun et al. discovered that CdTe QDs, a type of sensitizer, could boost the CL emission from the redox reaction of  $\text{SO}_3^{2-}$  with Ce (IV) in an acidic media [74]. The sensitized CL exhibited a size-dependent effect, with the CL effect increasing as the QDs sizes increased. They used the enhanced CL system for the determination of different chemical and biological compounds.

The 2-mercaptopropanoic acid-capped ZnS QDs were used for the CL improvement of the bisulfite-peroxide system in an acidic medium [23]. Mechanistically, QDs have a dual role: catalysts for the production of free radicals and energy acceptors from the excited  $\text{SO}_2^*$ . Lastly, oppositely charged QDs recombine to form excited states (Figure 3b). This given system is unique from other systems as it operates under acidic conditions rather than basic ones. Additionally, dilution with water enhanced the intensity, attributable to the occurrence of hydrolysis at a high concentration of bisulfite. The order of mixing of the reagents was noted to have an impact on the CL signals.

Chen et al. used plasmonic NPs to enhance the CL intensity of the sulfite- $\text{H}_2\text{O}_2$  system [75]. They elucidated the CL enhancement mechanism of the system (Figure 3c). Sun et al. employed  $\text{WS}_2$  nanosheets to produce CL from the  $\text{Fe}^{2+}/\text{SO}_3^{2-}$  system [76]. More  $\text{SO}_4^{\bullet-}$  radicals and significant intrinsic CL were generated by activating sulfite with a  $\text{Fe}^{2+}$  ion on 5 nm-thick  $\text{WS}_2$  nanosheets (Figure 3d). The improved CL increased the efficiency of pollutant degradation. High levels of  $\text{SO}_4^{\bullet-}$  and a little  $\bullet\text{OH}$  radicals were produced, which were then employed to directly reduce the organic contaminants.

To detect  $\text{SO}_3^{2-}$  specifically in particulate matter ( $\text{PM}_{2.5}$ ) samples, Li et al. employed Eu/ $\text{CeO}_2$  NPs [77]. A redox reaction between Eu/ $\text{CeO}_2$  and  $\text{SO}_3^{2-}$  produces the luminous intermediate  $\text{SO}_2^*$  (Figure 4a), which then stimulates Eu/ $\text{CeO}_2$  to get luminescence (Figure 4b).

$\text{CoFe}_2\text{O}_4$  NPs could catalyze the oxidation of luminol by dissolved oxygen to produce intense CL, as was reported by Zhang et al. [78]. The observed emitting species was the 3-aminophthalate anions (3-APA\*). The sulfite used had an inhibition effect at low concentrations but a contrary effect at higher concentrations. The devised method was applied for the trace analysis of sulfite in white wine.

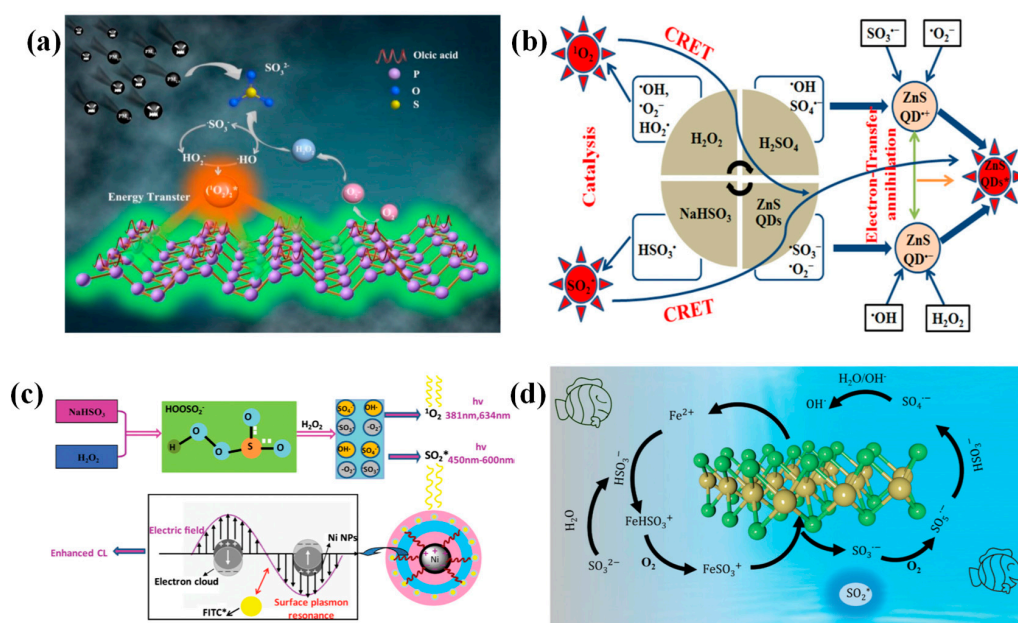


**Figure 3.** NMs enhanced sulfite CL systems. (a) Schematic of the OA-BP enhanced NaHSO<sub>3</sub> CL system. Reprinted with permission from [69], copyright 2019, American Chemical Society. (b) Proposed mechanism for the enhancement of sulfite-H<sub>2</sub>O<sub>2</sub> CL system by the ZnS QDs. Reprinted with permission from [23], copyright 2016, American Chemical Society. (c) The mechanism of plasmonic NPs enhanced the sulfite CL system. Reprinted with permission from [75], copyright 2013, Elsevier. (d) A schematic representation of CL and free radical transformation in the Fe (II)-sulfite system supported by WS<sub>2</sub> nanosheets. Reprinted with permission from [76], copyright 2020, Royal Society of Chemistry.

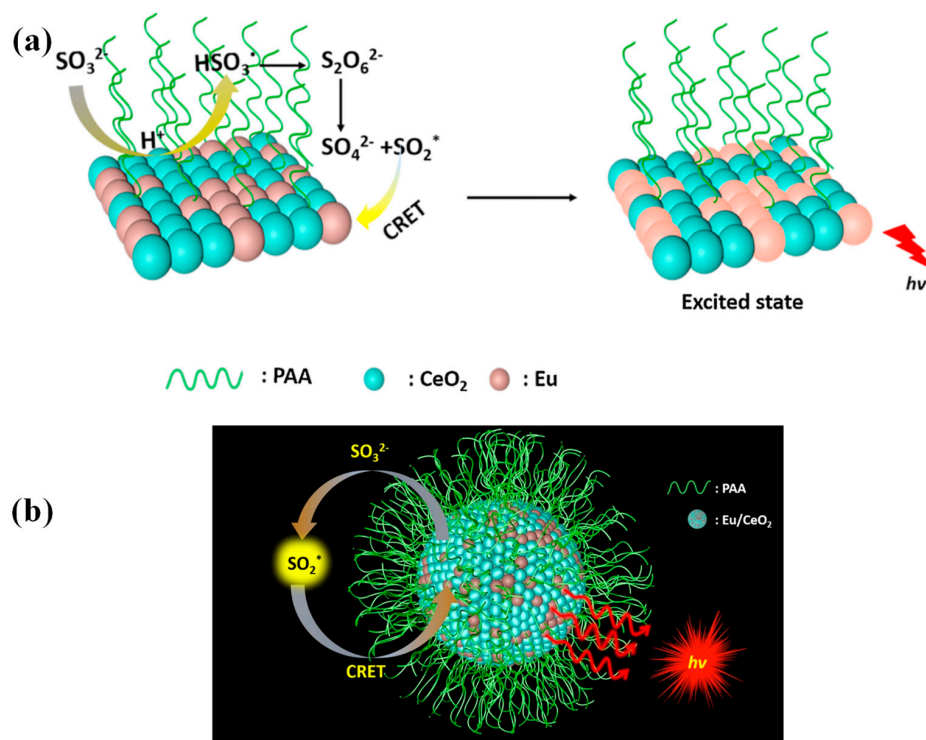


**Figure 4.** NMs assisted CRET CL system. (a) CL reaction mechanism of the sulfite-Eu/CeO<sub>2</sub> system in an acidic medium. (b) The CRET from SO<sub>2</sub><sup>\*</sup> to Eu/CeO<sub>2</sub> NPs. Reprinted with permission from [77], copyright 2021, Elsevier.

### 3.3. Metal Ions

Metal ions have the ability to either increase or decrease the emission intensity of a particular CL system. Li et al. used water-soluble CdTe nanocrystals to investigate the effect of metal ions on CL in the CdTe/H<sub>2</sub>O<sub>2</sub> system [34]. The study examined the influence of pH, CdTe particle sizes, and reagent concentration on the kinetics curve and CL intensity. The results indicated that Ba<sup>2+</sup>, Ca<sup>2+</sup>, Fe<sup>2+</sup>, Pb<sup>2+</sup>, and Cu<sup>2+</sup> increased the intensity of CL, while Cr<sup>3+</sup>, Ni<sup>2+</sup>, Zn<sup>2+</sup>, and Ag<sup>+</sup> decreased it under optimal conditions. Various metal ions have been used for the oxidation of S (IV) species. Zhang et al. explained the metal ion-induced catalytic oxidation of the S (IV) ion [79]. This study investigated the kinetics of the Fe (II)-induced catalytic oxidation of S (IV) at different iron concentrations. The reaction order for S (IV) oxidation towards O<sub>2</sub> and HSO<sub>3</sub><sup>-</sup> was found to be 0 and 1, respectively, while the reaction order towards Fe (II) varied depending on the iron concentration. The activation energy values were low at 30–50 °C but increased with an increase in ionic strength. Based on the analysis of radical mechanisms and reaction kinetics, a simplified model for the Fe (II)-induced catalytic oxidation of S (IV) was proposed. Liyan et al. used the Tb<sup>3+</sup> ion-enhanced KMnO<sub>4</sub>-sulfite system for the determination of gatifloxacin (GFLX) based on energy transfer from GFLX to Tb<sup>3+</sup> [80]. The method exhibited a linear range from 5.0 × 10<sup>-8</sup> to 8.0 × 10<sup>-6</sup> mol/L and a detection limit of 3.2 × 10<sup>-9</sup> mol/L. The method was successfully applied for the determination of GFLX in drug formulations, urine, and serum samples, with no interference from common excipients used in pharmaceutical preparations. Likewise, Yi et al. used the Tb<sup>3+</sup> ion to enhance the CL intensity of the KMnO<sub>4</sub>-sulfite system [81]. The work introduces a KMnO<sub>4</sub>/Na<sub>2</sub>SO<sub>3</sub> CL system that uses Tb<sup>3+</sup> as a sensitizer to detect the fluoroquinolones ENX and OFLX, resulting in very low detection limits. The weak CL emission from the system due to SO<sub>2</sub>\* was enhanced by the energy transfer from the SO<sub>2</sub>\* to the Tb<sup>3+</sup> fluoroquinolones chelate. The enhanced CL system was used for the determination of fluoroquinolones in pharmaceutical formulations and biological fluids, including urine samples, without any pre-handling but by appropriate sample dilution. The study also proposed a possible CL mechanism.

### 3.4. Complexes and Other Molecules Enhanced Sulfite CL Systems

The weak CL from the bisulfite and H<sub>2</sub>O<sub>2</sub> was enhanced by the addition of benzo[a]pyrene-7,10-quinone (7,10-BaPQ) by Li et al. [30]. The free radicals generated in the system cause a reduction of 7,10-BaPQ to semiquinone in the excited state resulting in an enhanced CL emission. The enhanced system was used for the determination of 7,10-BaPQ in airborne particulates (Figure 5a).

Zhang et al. used the Ru (II) complex (Ru-CHO) for the determination of hydrogen sulfite [82]. The aldehydic functionality of the Ru-CHO complex reacts with the hydrogen sulfite to form the Ru-SO complex resulting in CL enhancement (Figure 5b). The CL intensity linearly increases with the increase in the hydrogen sulfite concentration. The enhanced system was used for the recognition of hydrogen sulfite in wine and sugar samples.

Cao et al. enhance the CL intensity from the oxidation of sodium sulfite with KMnO<sub>4</sub> by Ru complex, with Ru (phen)<sub>3</sub><sup>2+</sup> as an acidic medium [83]. The final emission was from the Ru (II) complex. CL intensity was linearly proportional to the concentration of progesterone in the range of 0.1 to 6.0 ng/mL. The developed method was used to determine progesterone in pharmaceutical formulations. KBrO<sub>3</sub> is widely used in flour as a bleaching agent. However, many studies have shown that it has toxic effects on human health. Yan et al. used Na<sub>2</sub>SO<sub>3</sub>, quinine sulfate, and KBrO<sub>3</sub> CL systems in an acidic medium for the determination of KBrO<sub>3</sub> in flour [84]. The weak CL intensity from the reaction of the KBrO<sub>3</sub>-Na<sub>2</sub>SO<sub>3</sub> system was enhanced by quinine sulfate. The CL intensity increased linearly with an increase in KBrO<sub>3</sub> in the flour sample from a 7 × 10<sup>-6</sup> to 1 × 10<sup>-4</sup> mol/L range.

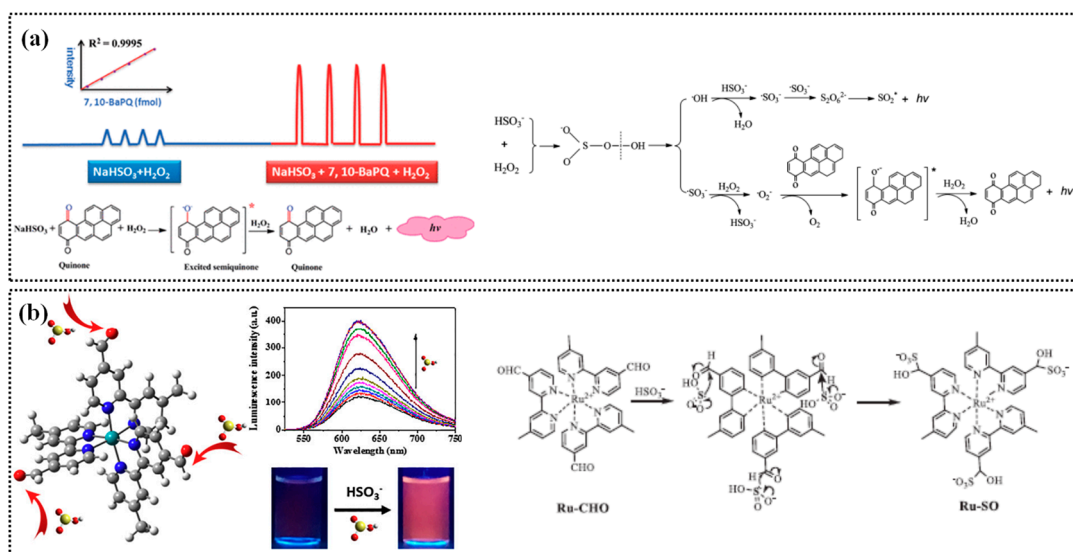


**Figure 5.** (a) Mechanism of enhancement and determination of 7,10-BaPQ in NaHSO<sub>3</sub>-H<sub>2</sub>O<sub>2</sub> system. Reprinted with permission from [30], copyright 2012, American Chemical Society. (b) The CL enhancement mechanism of Ru(II) complex with hydrogen sulfite. Reprinted with permission from [82], copyright 2018, Elsevier.

The determination of SO<sub>2</sub> and sulfite is important as it has been used in food products. Meng et al. used the Ru(bipy)<sub>3</sub><sup>2+</sup> complex enhanced KMnO<sub>4</sub>-SO<sub>3</sub><sup>2-</sup> CL system for the determination of sulfite in sugar and SO<sub>2</sub> in the air [85]. They tried different surfactants for the enhancement of the CL system. By this CL detection method, the determination of sulfite in a concentration range from 5.0 × 10<sup>-8</sup> to 1.25 × 10<sup>-4</sup> mol/L with a LOD of 2.5 × 10<sup>-8</sup> mol/L can be done. This method has been successfully applied to the determination of sulfite in sugar and sulfur dioxide in air using triethanolamine (TEA) as an absorbent. Wu et al. used the Ru(bipy)<sub>3</sub><sup>2+</sup> complex enhanced KBrO<sub>3</sub>-Na<sub>2</sub>SO<sub>3</sub> CL system for the determination of sulfite in sugar and SO<sub>2</sub> in the air [86]. Sulfite can be identified in the range of (0.0500–5.00) × 10<sup>-6</sup> mol/L using the emission that results from sulfite-induced autoxidation of the Ni(II)/tetraglycine complex in the presence of luminol [87]. The method has a LOD of 2.8 × 10<sup>-8</sup> mol/L and a relative standard deviation of 4.6% for 1 × 10<sup>-7</sup> mol/L sulfite in five repeated measurements. The method has been successfully applied for the determination of sulfite in wine, juices, white sugar, and rainwater using a gas-diffusion unit for sulfite extraction.

Huang et al. determined the sulfite by the combined effect of Rh6G and Tween 80 in an acidic environment based on auto-oxidation sensitized by rhodamine 6G in the presence of Tween 80 surfactant micelles [88]. The linear range for sulfite concentration is 0.05–10 mg/L with a detection limit (3σ) of 0.03 mg/L and a relative standard deviation of less than 5% (n = 11). The system has been successfully applied for the determination of total sulfite in beverages, and the possible reaction mechanism has been discussed. He et al. also used the CL system for the determination of sulfite in food products [89]. A new microflow injection analysis (μFIA) system on a chip for sulfite determination based on a CL reaction between Ce(IV) and sulfite sensed by Rh6G and Tween 80 in an acid medium was presented. The system has channels that are 200 μm wide and 150 μm deep with a reaction area volume of 1.80 μL, and reagents are monitored by an injection pump at a rate of 50 μL/min. The linear range of sulfite concentration is 1.0–60 μg/mL with a detection limit of 0.5 μg/mL, and the method has good reproducibility with a relative standard deviation of 3.0% (n = 7) for 20 μg/mL of sulfite. The method has been successfully applied for the determination of sulfite in food. The oxidation of sulfite in the presence of Rh6G in an acidic medium produces weak CL. Tween 80 enhanced the weak CL of this system [90]. The amphiphilic Tween 80 surfactant molecules form the micelles, which protect the excited state, and thus

enhancement in CL was noted. The enhanced system was used for the determination of sulfite in the range of 0.01 to 5 mg/L, with 0.01 mg/L LOD.

Zhang et al. used papaverine to enhance the CL intensity of the sulfite system in the presence of acidic Ce (IV) [91]. Ce (IV) causes the oxidation of the papaverine to form its radical. CL enhancement was directly proportional to the concentration of papaverine in pharmaceutical formulations and biological fluids. Likewise, Ali et al. used zolpidem to enhance the Na<sub>2</sub>SO<sub>3</sub>-KMnO<sub>4</sub> CL system in the acidic medium [92]. Zolpidem is used as a short-term treatment for insomnia. The enhanced CL system was used for the determination of zolpidem in pharmaceutical formulations and human plasma. The oxidation of sulfite results in CL. Pauls et al. used 3-cyclohexylaminopropanesulfonic acid to sensitize the CL of sulfite [3]. They suggested that the presence of the cyclohexyl ring sensitizes the reaction.

The sensitizing impact of sulfite on the known CL emission produced by the oxidation of luminol in alkaline media was used by Navarro et al. to develop a sensitive CL method for the measurement of sulfite in wine [93].

By comparing the usage of riboflavin and 3-cyclohexylaminopropanesulphonic acid (CAPS), Tamrah et al. were able to improve the sensitivity of the sulfite measurement in a flow injection process based on the CL produced by permanganate oxidation in an acidic solution [94]. Similar to this, Zhang et al. created an anion exchange column-based CL flow sensor for sulfite by electrostatically immobilizing KMnO<sub>4</sub> and riboflavin phosphate [95]. Likewise, based on electrostatically immobilized luminol on an anion exchange column, a unique CL flow system for sulfite was developed [96]. The system has been successfully utilized to determine the presence of sulfur dioxide in the air and could be reused for more than 50 h.

Yamada et al. identified sulfite by the CL emission it produces when permanganate oxidizes it in an acidic solution in the presence of riboflavin phosphate or brilliant sulfaflavine [97]. The sulfite and permanganate CL, which result from excited SO<sub>2</sub><sup>\*</sup>, give rise to weak CL. The excited molecules' energy is easily transferred to the fluorescent molecules that have been introduced to the system.

Li et al. designed a sulfite-assisted Ce (IV)-MOF CL system [98]. The free radicals were generated from the reduction of sulfite on the surface of Ce (IV)-MOF. These free radicals result in the emissive SO<sub>2</sub><sup>\*</sup> as an intermediate. The intermediate then transfers its energy to the added dye molecules (Nile blue and rhodamine B) through CRET with enhanced CL emission (Figure 6a). Based on the enhanced CL system, they designed a CL sensor for sulfite in PM<sub>2.5</sub>.

Sun et al. created a CL probe, APDI (N,N'-di(propylethylenediamine)-perylene-3,4,9,10-tetracarboxylic diimide), to detect the •OH radical among a variety of other radicals [17]. The Fenton system was used to generate the •OH radical. The sulfite was used as a reducing agent for the conversion of Fe<sup>3+</sup> to Fe<sup>2+</sup> ions in the system. The APDI was used to specifically detect the generated •OH radicals in the system. The generated radicals in the system were used for the degradation of bisphenol A, as a contaminant, through AOPs in environmental samples (Figure 6b).

### 3.5. Solvent-Enhanced Sulfite CL Systems

Li et al. used alcoholic solvents to enhance the weak CL from the sulfite-H<sub>2</sub>O<sub>2</sub> system [54]. They enhanced the CL intensity by using alcoholic solvents with two to five carbon atoms. The n-butanol is the most suitable carbon for carbon cage formation, and among the used alcohols, it results in the highest CL intensity (Figure 7). The alcoholic solvent forms the solvent cage, somewhat similar to micelles in water. The CL-enhancing effect was attributed to the following three main reasons; (i) the solubilization effect of the micellar system, (ii) the concentration of the CL reagents at the micellar system due to the electrostatic effects, and (iii) the micellar system circumvents the quenching of emitting species and protects the radicals.

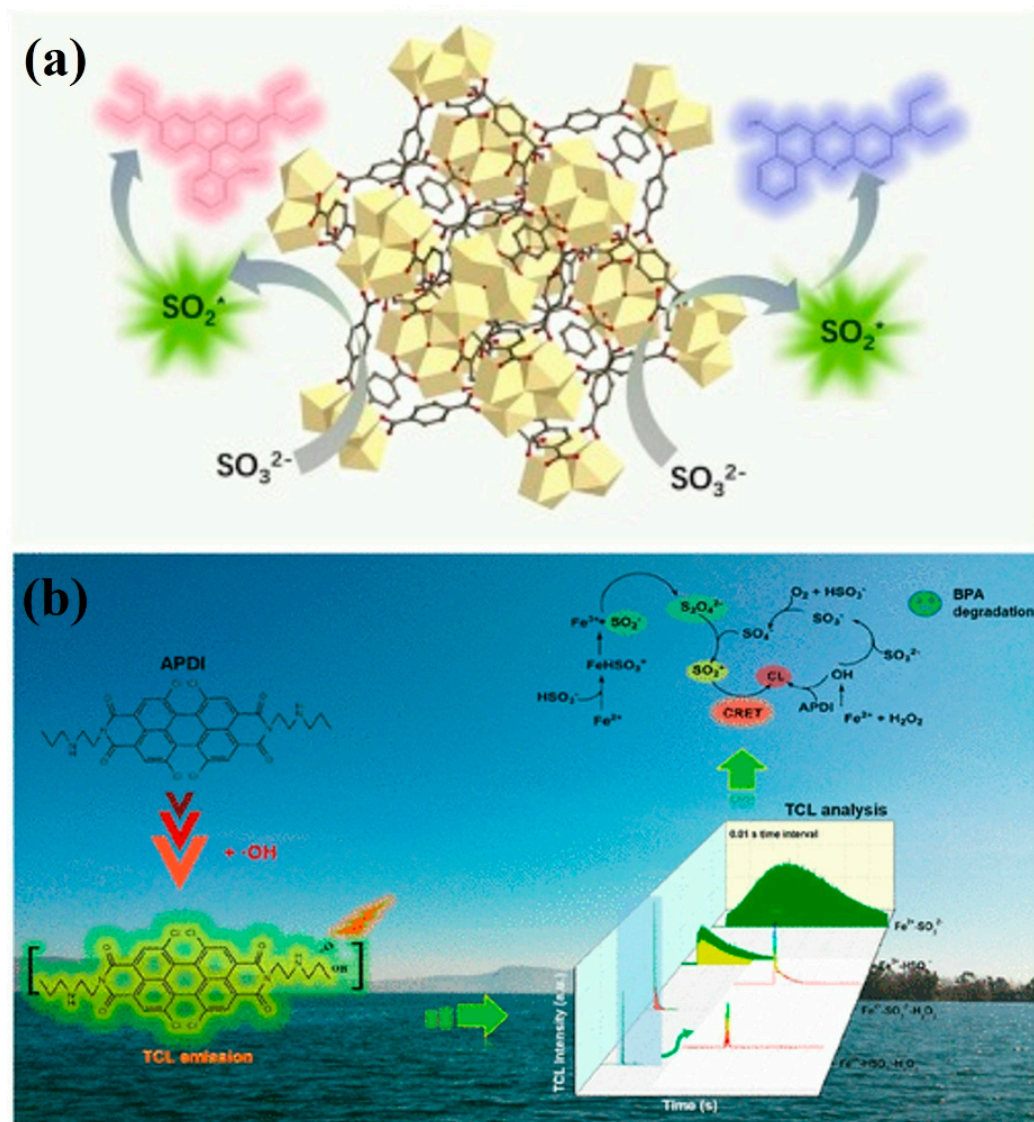


**Figure 6.** (a) The mechanism of generation of  $\text{SO}_2^*$  on the Ce (IV)-MOF system as well as the energy transfer mechanism in the presence of dye molecules. Reprinted with permission from [98], copyright 2023, Elsevier. (b) Generation and detection of  $\bullet\text{OH}$  radical in sulfite supported the Fenton system and its utilization of the degradation of organic pollutants through AOPs. Reprinted with permission from [17], copyright 2022, American Chemical Society.

Not much research work on the solvent effect of the sulfite system has been reported. Conversely, Zhang et al. described a CL system for the determination of sodium dodecylbenzene sulfonate (SDBS) using an  $\text{IO}_4^-$ - $\text{H}_2\text{O}_2$  reaction, where various surfactants enhance CL intensity, particularly SDBS [99]. The method has a  $3\sigma$  detection limit of  $3.2 \times 10^{-8}$  g/mL, and a relative standard deviation of 1.6% at  $1.0 \times 10^{-6}$  g/mL for 11 determinations and has been successfully used to determine SDBS in detergents.

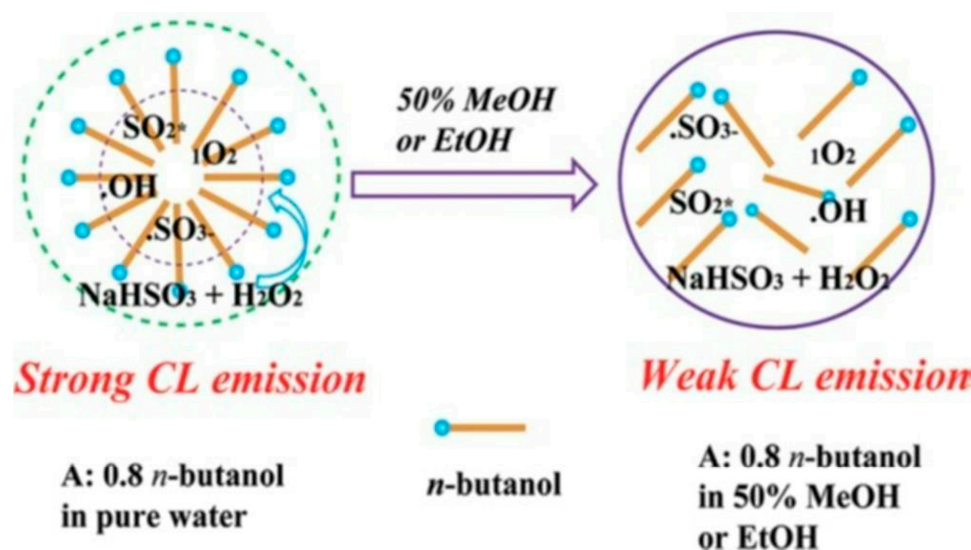


**Figure 7.** The enhancement effect of *n*-butanol on the CL intensity of  $\text{NaHSO}_3\text{-H}_2\text{O}_2$  CL system. Reprinted with permission from [54], copyright 2012, American Chemical Society.

#### 4. Analytical Applications

A variety of NP-assisted CL techniques and sensor devices expand the analytical value of CL detection, particularly with regard to selectivity problems observed more obviously when sample complexity or the number of target analytes is high [42]. In the rapidly expanding field of nanotechnology, the QDs are one of the most important developments. They were first proposed as luminous biological markers, but analytical chemistry is finding new and significant uses for them [100]. The CL methods have been widely used as CL immunosensor [101–104] as well as a sensor for reagents of environmental concerns [105,106]. In comparison, the use of CL detection for sulfite offers a different set of advantages, including high sensitivity, low detection limits, and the ability to detect other analytes besides sulfite. While fluorescent probes may be more suitable for real-time imaging and non-invasive detection [107], CL detection may be better suited for certain analytical applications. Ultimately, the choice of detection method will depend on the specific needs of the application at hand.

The sulfites are used as a preservative in the pharmaceutical and food industries. So various methods for sulfite detection [11,108] gained the utmost significance to assure food quality [109]. The inhibited CL systems are usually applied for the determination of trace analysis, specifically for the detection of a minute quantity of organic and inorganic compounds. In this context, the CL-based method, when combined with flow-injection analysis (FIA), is a quick, easy, and repeatable detection process and can be effectively used to detect many different substances in a wide range of matrices [93]. The detection principle is that compound or material must either increase or decrease CL intensity.

As said earlier, for sulfite detection of complex materials, designing a CL sensing platform with high sensitivity and selectivity is crucial [77]. In food safety, environmental monitoring, medical diagnostics, and public health assurance sectors, there is an urgent demand for rapid on-site detection with high sensitivity and specificity [110]. One such system is the detection of  $\text{H}_2\text{O}_2$  [111] in environmental samples using sulfite-amplified CL [112]. The different reagents determined in various samples by the sulfite-based CL systems are summarized in Table 1 and are under discussion in the following sections.

##### 4.1. Biological and Chemical Analysis

Proteins such as cytochrome *c*, hemoglobin, and myoglobin, and organic substances composed of OH,  $\text{NH}_2$ , or SH groups readily interact with CdTe QDs suppressing the CL signal of the  $\text{Ce(IV)-SO}_3^{2-}\text{-CdTe}$  QDs system, and hence can be used for the detection of these substances [74].

#### 4.2. Food and Consumer Products

The quality and safety of food are among major concerns nowadays. Population growth and the worldwide industrial revolution have increased interest in and consistent demand for food. Food analysis faces hurdles because of the presence of low-abundant ingredients such as preservatives, pesticide residues, allergies, toxins, metals with toxicity, and other additives with varying degrees of reactivity and behavior [113]. Liu et al. reviewed in detail the application of CL in food analysis [5].

Bromate is toxic to humans and other biotic components of the environment. Li et al. successfully determined bromate in a drinking water sample by the CDs-sulfite CL system [66]. Sulfite-based CL has been used for the determination of  $\text{KBrO}_3$  in flour [84]. Likewise, sulfite in sugar [85,86], white wines [78], and hydrogen sulfite in sugar and wine were determined by CL methods [82]. The sensitizing effect of sulfite on alkaline luminol/permanganate reactions allowed for a quick CL measurement of sulfite in wine [93]. Sulfite levels in wine, juices, white sugar, and rainwater have all been determined with success using the CL technique [87]. Zhang et al. noted that the N,S-GQD- $\text{NaHSO}_3$ - $\text{NaClO}$  system is noticeably diminished by folic acid (FA; vitamin B9). A sensitive CL approach was developed for the detection of FA in food samples based on this discovery [67].

#### 4.3. Pharmaceutical and Clinical Analysis

The CL application in drug screening was studied in detail by Roda et al. [114]. Sulfite-based CL has been used for the determination of Zolpidem in pharmaceutical formulations and human plasma [92], gatifloxacin in pharmaceutical formulations, urine and serum samples [80], and norfloxacin in human urine [70]. Various CL systems used by different researchers are papaverine enhanced sulfite CL system for the determination of papaverine in biological fluid and pharmaceutical formulation [91], the  $\text{Tb}^{3+}$  enhanced  $\text{KMnO}_4$ -sulfite CL system for the determination of fluoroquinolones in pharmaceutical formulations and biological fluids [81], CdS QDs enhanced  $\text{Ce(IV)-SO}_3^{2-}$  CL system for cetirizine in pharmaceutical formulations [73] and Ag NPs enhanced  $\text{Ce(IV)-SO}_3^{2-}$  CL system in eyedrops [71]. Mohammad et al. used a simple and accurate CL approach combined with flow-injection technology to determine NAP [72]; this was commercially used to measure the presence of NAP in NAP pills.

#### 4.4. Agricultural and Environmental Applications

The CL analysis has also been applied for the determination of different compounds and molecules of the environment and of agricultural significance (Table 1). Polyaromatic hydrocarbons are organic compounds of environmental concern [30] as they produce reactive oxygen species (ROS), which have detrimental effects on both the structure and functioning of biological cells. So, the development of reliable and sensitive analytical methods for the determination of these environmentally hazardous compounds is of the utmost importance. CL has been used for the determination of  $\text{SO}_2$  in the air [85,86], sulfite in  $\text{PM}_{2.5}$  [69], 7,10-BaPQ in airborne particulates [30], and  $\text{Fe}^{3+}$  ions in real water samples [68]. Li et al. successfully used it to detect  $\text{SO}_3^{2-}$  specifically in  $\text{PM}_{2.5}$  samples by the CL reaction from sulfite oxidation on the interface of  $\text{Eu/CeO}_2$  NPs [77]. The improved CL increased the efficiency of pollutant degradation. High levels of  $\text{SO}_4^{\bullet-}$  and a little  $\bullet\text{OH}$  radicals were produced on the surface of  $\text{WS}_2$  nanosheets from the CL reaction of  $\text{Fe}^{2+}$ , and the sulfite system was employed to directly reduce organic contaminants [76]. Li et al. designed a CL sensor for sulfite by a dye-sensitized  $\text{Ce(IV)-MOF}$  system. The designed sensor was applied for the determination of sulfite in  $\text{PM}_{2.5}$  samples [98]. Monitoring the  $\bullet\text{OH}$  radical is essential for understanding the workings of AOPs and evaluating how well they work to degrade organic pollutants. Sun et al. designed a CL sensor for the detection of the  $\bullet\text{OH}$  radical among other radicals for the degradation of organic contaminants through the AOPs process [17].

**Table 1.** Summarizes the different enhancers used to enhance the CL emission of sulfite systems. The mechanism of the systems and the emitting species in the system, along with its uses for the determination of different reagents in various samples, are also covered. The data was arranged from old to new.

Enhancer	CL Systems	Mechanism	Emitting Species	Analytes	Samples	Remarks	Publishing Year	Ref.
Ru(bipy) <sub>3</sub> <sup>2+</sup>	KBrO <sub>3</sub> -SO <sub>3</sub> <sup>2-</sup>	Ru(bipy) <sub>3</sub> <sup>2+</sup> is the emitting species in the enhanced CL system	Ru(bipy) <sub>3</sub> <sup>2+</sup>	Sulfite and SO <sub>2</sub>	Sugar and Air	The CL intensity linearly increases with an increase in the analyte concentration	1998	[86]
Surfactants	Ru(bipy) <sub>3</sub> <sup>2+</sup> -KMnO <sub>4</sub> -SO <sub>3</sub> <sup>2-</sup>	Ru(bipy) <sub>3</sub> <sup>2+</sup> is the emitting species in the enhanced CL system	Ru(bipy) <sub>3</sub> <sup>2+</sup>	Sulfite and SO <sub>2</sub>	Sugar and Air	The CL intensity linearly increases with an increase in the analyte concentration	1999	[85]
Rh6G and Tween 80	Na <sub>2</sub> SO <sub>3</sub>	SO <sub>2</sub> <sup>*</sup> transfers its energy to the Rh6G	Rh6G	Sulfite	Beverages	The CL intensity linearly increases with an increase in the sulfite concentration	1999	[88]
Tb <sup>3+</sup>	KMnO <sub>4</sub> sulfite	The Tb <sup>3+</sup> ions form a chelate with the fluoroquinolones and result in the enhanced CL	Tb <sup>3+</sup>	fluoroquinolones	Pharmaceutical formulation and biological fluids	The energy from the SO <sub>2</sub> <sup>*</sup> is transferred to the Tb <sup>3+</sup> chelates and results in high CL emission	2003	[81]
papaverine	Sulfite-Ce (IV)	The papaverine oxidation by Ce (IV) causes the high CL intensity	SO <sub>2</sub> <sup>*</sup>	Papaverine	Pharmaceutical formulation and biological fluids	The papaverine radical is formed during the reaction	2004	[91]
Rh6G and Tween 80	Ce (IV)-SO <sub>3</sub> <sup>2-</sup>	The enhancers were excited by the reaction products	Rh6G	Sulfite	Food samples	The CL intensity linearly increases with an increase in the sulfite concentration	2005	[89]
CdTe QDs	Ce (IV)-SO <sub>3</sub> <sup>2-</sup>	The CdTe QDs enhance the CL intensity of the system	CdTe QDs	Chemical and biological compounds	-	-	2008	[74]
Au NPs	Na <sub>2</sub> SO <sub>3</sub> <sup>-</sup> Ce (IV)	Au NPs catalyze the production of the SO <sub>2</sub> <sup>*</sup> , which results in enhanced CL emission	SO <sub>2</sub> <sup>*</sup>	Norfloxacin	Human urine	The SO <sub>2</sub> <sup>*</sup> transfers its energy to the norfloxacin on the surface of the Au NPs	2009	[70]
Sulfite	KMnO <sub>4</sub> luminol	-	-	Sulfite	Wine samples	The sulfite has enhancing effect on the system	2010	[93]
Ag NPs	Ce (IV)-SO <sub>3</sub> <sup>2-</sup>	The Ag NPs catalyze the CL reaction of Ce (IV)-SO <sub>3</sub> <sup>2-</sup>	Tb <sup>3+</sup>	Norfloxacin	Eyedrops	The energy of SO <sub>2</sub> <sup>*</sup> is transferred to the Tb <sup>3+</sup> ion, and the final emission takes place from it	2010	[71]

Table 1. Cont.

Enhancer	CL Systems	Mechanism	Emitting Species	Analytes	Samples	Remarks	Publishing Year	Ref.
7,10-BaPQ	NaHSO <sub>3</sub> -H <sub>2</sub> O <sub>2</sub>	The free radicals reduce 7,10-BaPQ to semiquinone in the excited state	Semiquinoline	7,10-BaPQ	Airborne particulates	The CL intensity linearly increases with an increase in 7,10-BaPQ concentration	2012	[30]
Eu <sup>3+</sup>	Ce (IV)-Na <sub>2</sub> S <sub>2</sub> O <sub>4</sub>	The Eu <sup>3+</sup> ions catalyze the CL reaction of Ce (IV)-Na <sub>2</sub> S <sub>2</sub> O <sub>4</sub>	Eu <sup>3+</sup>	Naproxen	Pharmaceutical formulation	The SO <sub>2</sub> * transfers its energy to the Eu <sup>3+</sup> ions to result in enhanced emission	2012	[72]
CoFe <sub>2</sub> O <sub>4</sub>	Luminol-SO <sub>3</sub> <sup>2-</sup>	Luminol is oxidized by the dissolved oxygen in the presence of CoFe <sub>2</sub> O <sub>4</sub> NPs	3APA*	Sulfite	White wines	The sulfite has an inhibition effect, while at higher concentrations, it has an enhancing effect on CL intensity	2013	[78]
Tb <sup>3+</sup>	Na <sub>2</sub> SO <sub>3</sub> -KMO <sub>4</sub>	The Tb <sup>3+</sup> ion forms a complex with the gatifloxacin, which may result in CL enhancement	Tb <sup>3+</sup>	Gatifloxacin	Pharmaceutical formulation, urine, and serum samples	CL intensity is linearly proportional to the gatifloxacin concentrations in these samples	2014	[80]
Quinine sulfate	KBrO <sub>3</sub> -Na <sub>2</sub> SO <sub>3</sub>	Quinine sulfate could be excited by the CL reaction	Quinine sulfate	KBrO <sub>3</sub>	Flour	The intermediates of the CL reaction transfer their energy to Quinine sulfate	2016	[84]
ZnS QDs	NaHSO <sub>3</sub> -H <sub>2</sub> O <sub>2</sub>	The different free radicals produced in the systems result in the enhancement of the CL	ZnS QDs	-	-	The water helps in the hydrolysis of the NaHSO <sub>3</sub> , which further enhances the CL	2016	[23]
CdS QDs	Ce (IV)-SO <sub>3</sub> <sup>2-</sup>	The CdS QDs enhance the CL intensity of the system	CdS QDs	-	Cetirizine injection	The Cetirizine further enhances the CL intensity	2016	[73]
Zolpidem	Na <sub>2</sub> SO <sub>3</sub> -KMO <sub>4</sub>	SO <sub>2</sub> * is formed as an emitting species in the reaction mixture	SO <sub>2</sub> *	Zolpidem	Pharmaceutical formulation and human plasma	Zolpidem is oxidized by the KMnO <sub>4</sub> , which then excites the SO <sub>2</sub>	2017	[92]
CDs	BrO <sub>3</sub> <sup>-</sup> -Na <sub>2</sub> SO <sub>3</sub> -	Electrons and holes were injected into the CDs by the redox reaction	CDs	Bromate	Water	The CL intensity linearly increases with an increase in bromate in drinking water	2018	[66]
Ru(II) complex	Hydrogen sulfite	Ru-CHO complex reacts with sulfite to form Ru-SO complex with an enhanced CL emission	Ru(II) complex	Hydrogen sulfite	Sugar and wine	The CL intensity linearly increases with an increase in hydrogen sulfite in food samples	2018	[82]

Table 1. Cont.

Enhancer	CL Systems	Mechanism	Emitting Species	Analytes	Samples	Remarks	Publishing Year	Ref.
NGQDs	Na <sub>2</sub> SO <sub>3</sub> -KMnO <sub>4</sub>	The dissolved oxygen was converted to H <sub>2</sub> O <sub>2</sub> and •OOH radicals by the NGQDs	NGQDs	Fe <sup>3+</sup>	Water samples	The Fe <sup>3+</sup> ions form a chelate with the phenolic functionalities of the NGQDs and thus decrease CL intensity	2018	[68]
OA-BP QDs	Na <sub>2</sub> SO <sub>3</sub>	<sup>1</sup> O <sub>2</sub> and (O <sub>2</sub> ) <sub>2</sub> <sup>*</sup> transfer their energy to the OA-BP QDs	OA-BP QDs	Sulfite	PM <sub>2.5</sub>	CL intensity is linearly proportional to the sulfite in PM <sub>2.5</sub>	2019	[69]
N,S-GQD, N-GQD, GQD	NaHSO <sub>3</sub> -NaClO, NaHSO <sub>3</sub> -H <sub>2</sub> O <sub>2</sub> and NaHSO <sub>3</sub> -KMnO <sub>4</sub>	SO <sub>2</sub> <sup>*</sup> transfers its energy to the N,S-GQD and thus results in enhanced CL emission	N,S-GQD	Folic acid	Food samples	Folic acid causes a linear decrease in CL emission, and thus, it is determined	2019	[67]
S,N-CDs	Mn-Na <sub>2</sub> SO <sub>3</sub>	SO <sub>2</sub> <sup>*</sup> was formed from the reaction of Mn(IV) with SO <sub>3</sub> <sup>2-</sup>	S, N-CDs	Oxytetracycline	Milk and water	The SO <sub>2</sub> <sup>*</sup> transfers its energy to the CDs to result in enhanced emission	2020	[65]
WS <sub>2</sub> nanosheets	Fe (II)-sulfite	The WS <sub>2</sub> nanosheets cause the conversion of Fe (II)/Fe(III) species and result in the high production of free radicals	SO <sub>2</sub> <sup>*</sup>	Reduction	Organic contaminants	The elevated production of free radicals causes the reduction of organic contaminants	2020	[76]
Eu/CeO <sub>2</sub> NPs	Sulfite-Eu/CeO <sub>2</sub>	SO <sub>2</sub> <sup>*</sup> was formed at the interface of Eu/CeO <sub>2</sub> NPs	Eu/CeO <sub>2</sub> NPs	Sulfite	PM <sub>2.5</sub>	The SO <sub>2</sub> <sup>*</sup> transfers its energy to Eu/CeO <sub>2</sub> NPs through CRET	2021	[77]
sulfite	Fe <sup>2+</sup> -H <sub>2</sub> O <sub>2</sub>	The sulfite was used as a reducing agent for the easy conversion of Fe <sup>3+</sup> to Fe <sup>2+</sup>	-	Bisphenol A	Organic contaminants	APDI is specifically designed to detect the •OH radical in the system	2022	[17]
Nile blue and rhodamine B	Ce (IV)-MOF-sulfite	SO <sub>2</sub> <sup>*</sup> was formed from the reduction of sulfite at the interface of Ce (IV)-MOF	Nile blue and rhodamine B	Sulfite	PM <sub>2.5</sub>	The SO <sub>2</sub> <sup>*</sup> transfers its energy to Nile blue and rhodamine B through CRET with enhanced CL emission	2023	[98]

<sup>1</sup> CL emission of sulfite systems. The mechanism of the systems and the emitting species in the system, along with its uses for the determination of different reagents in various samples, are also covered.

## 5. Conclusions and Future Perspectives

The review emphasized the detailed behavior of CL of the systems involving sulfite species. The CL response of the sulfite-containing CL systems can be enhanced with the help of diverse enhancers, i.e., NMs, QDs, CDs, metal ions, solvents, complexes, and different other molecules. The poor selectivity, in most cases, and the modes of understanding of the mechanism of the CL systems are the main hurdles in their practicality. Most researchers agreed upon a linear link between free radicals' generation and CL response. In this context, the role of distinctive enhancers is vital either to trigger free radicals' generation or to stabilize the intermediate responsible for the emission of CL.

The introduction of NMs to the CL system improved the CL intensity and, thus, the selectivity and sensitivity of the systems for various applications. The use of NMs in the CL systems had high CL intensity compared to the traditional systems and thus improved the sensitivity for different reagents. The CL has the inheritance advantage to lower the detection limit for analysis due to no interferences from the light as no excitation is used in CL. These and many more factors cause the lower detection of various reagents in environmental, biological, food, forensic, pharmaceutical, agricultural, and environmental analysis.

This review will give new insight into the search for a catalyst for the enhancement of the CL systems. Secondly, the detailed mechanism of the sulfite-based CL systems will help in the selection of the reagents and enhancers to boost the CL possession of the respective CL systems. Lastly, it will also broaden the application of the enhanced CL systems in various fields.

**Funding:** This research received no external funding.

**Institutional Review Board Statement:** Not applicable.

**Informed Consent Statement:** Not applicable.

**Acknowledgments:** The authors acknowledge the research of all the researchers whose works have been cited and have contributed to the advancement of this area.

**Conflicts of Interest:** The authors declare no conflict of interest.

## References

1. Fan, X.; Su, Y.; Deng, D.; Lv, Y. Carbon nitride quantum dot-based chemiluminescence resonance energy transfer for iodide ion sensing. *RSC Adv.* **2016**, *6*, 76890–76896. [[CrossRef](#)]
2. Garcia-Campana, A.M.; Baeyens, W.R.; Zhang, X. *Chemiluminescence-Based Analysis: An Introduction to Principles, Instrumentation, and Applications*; CRC Press: Boca Raton, FL, USA, 2001; p. 59.
3. Paulls, D.A.; Townshend, A. Enhancement by cycloalkanes of the chemiluminescent oxidation of sulfite. *Analyst* **1996**, *121*, 831–834. [[CrossRef](#)]
4. Dou, X.; Shah, S.N.A.; Lin, J.-M. *Introduction of Ultra-Weak Chemiluminescence*; Springer: Berlin/Heidelberg, Germany, 2022; p. 1. [[CrossRef](#)]
5. Liu, M.; Lin, Z.; Lin, J.-M. A review on applications of chemiluminescence detection in food analysis. *Anal. Chim. Acta* **2010**, *670*, 1–10. [[CrossRef](#)] [[PubMed](#)]
6. Zhou, Y.; Xing, G.; Chen, H.; Ogawa, N.; Lin, J.M. Carbon nanodots sensitized chemiluminescence on peroxomonosulfate-sulfite-hydrochloric acid system and its analytical applications. *Talanta* **2012**, *99*, 471. [[CrossRef](#)] [[PubMed](#)]
7. Baeyens, W.R.G.; Schulman, S.G.; Calokerinos, A.C.; Zhao, Y.; García Campaña, A.M.; Nakashima, K.; De Keukeleire, D. Chemiluminescence-based detection: Principles and analytical applications in flowing streams and in immunoassays. *J. Pharm. Biomed. Anal.* **1998**, *17*, 941–953. [[CrossRef](#)] [[PubMed](#)]
8. Chen, H.; Lin, L.; Li, H.; Lin, J.-M. Quantum dots-enhanced chemiluminescence: Mechanism and application. *Coord. Chem. Rev.* **2014**, *263–264*, 86–100. [[CrossRef](#)]
9. Lin, J.-M.; Lu, C.; Chen, H. *Ultra-Weak Chemiluminescence*; Springer: Berlin/Heidelberg, Germany, 2022.
10. Zuo, M.; Qian, W.; Hao, M.; Wang, K.; Hu, X.-Y.; Wang, L. An AIE singlet oxygen generation system based on supramolecular strategy. *Chin. Chem. Lett.* **2020**, *32*, 1381–1384. [[CrossRef](#)]
11. Bener, M.; Şen, F.B.; Apak, R. Novel pararosaniline based optical sensor for the determination of sulfite in food extracts. *Spectrochim. Acta Part A Mol. Biomol. Spectrosc.* **2019**, *226*, 117643. [[CrossRef](#)]
12. Chen, S.; Hou, P.; Wang, J.; Song, X. A highly sulfite-selective ratiometric fluorescent probe based on ESIPT. *RSC Adv.* **2012**, *2*, 10869–10873. [[CrossRef](#)]
13. Sapers, G. Browning of foods: Control by sulfites, antioxidants, and other means. *Food Technol.* **1993**, *47*, 75.

14. Abdel-Latif, M.S. New Spectrophotometric Method for Sulfite Determination. *Anal. Lett.* **1994**, *27*, 2601–2614. [[CrossRef](#)]
15. Güçlü, K.; Altun, M.; Özyürek, M.; Karademir, S.E.; Apak, R. Antioxidant capacity of fresh, sun-and sulphited-dried Malatya apricot (*Prunus armeniaca*) assayed by CUPRAC, ABTS/TEAC and folin methods. *Int. J. Food Sci. Technol.* **2006**, *41*, 76. [[CrossRef](#)]
16. Xiao, J.; Li, R.; Dong, H.; Li, Y.; Li, L.; Xiao, S.; Jin, Z. Activation of sulfite via zero-valent iron-manganese bimetallic nano-materials for enhanced sulfamethazine removal in aqueous solution: Key roles of Fe/Mn molar ratio and solution pH. *Sep. Purif. Technol.* **2022**, *297*, 121479. [[CrossRef](#)]
17. Sun, M.; Song, H.; Xie, X.; Yang, W.; Su, Y.; Lv, Y. Transient Chemiluminescence Assay for Real-Time Monitoring of the Processes of  $\text{SO}_3^{2-}$ -Based Advanced Oxidation Reactions. *Environ. Sci. Technol.* **2022**, *56*, 3170–3180. [[CrossRef](#)]
18. Maiti, B.K. Cross-talk Between (Hydrogen)Sulfite and Metalloproteins: Impact on Human Health. *Chem.—A Eur. J.* **2022**, *28*, e202104342. [[CrossRef](#)]
19. Chen, H.; Li, R.; Lin, L.; Guo, G.; Lin, J.-M. Determination of l-ascorbic acid in human serum by chemiluminescence based on hydrogen peroxide–sodium hydrogen carbonate–CdSe/CdS quantum dots system. *Talanta* **2010**, *81*, 1688–1696. [[CrossRef](#)]
20. Liu, J.; Chen, H.; Lin, Z.; Lin, J.-M. Preparation of Surface Imprinting Polymer Capped Mn-Doped ZnS Quantum Dots and Their Application for Chemiluminescence Detection of 4-Nitrophenol in Tap Water. *Anal. Chem.* **2010**, *82*, 7380–7386. [[CrossRef](#)]
21. Dasgupta, P.K. The importance of atmospheric ozone and hydrogen peroxide in oxidizing sulphur dioxide in cloud and rain water: Further discussion. *Atmos. Environ.* **1980**, *14*, 272–275. [[CrossRef](#)]
22. Flockhart, B.D.; Ivin, K.J.; Pink, R.C.; Sharma, B.D. The nature of the radical intermediates in the reactions between hydroperoxides and sulphur dioxide and their reaction with alkene derivatives: Electron spin resonance study. *J. Chem. Soc. D Chem. Commun.* **1971**, 2243, 339–340. [[CrossRef](#)]
23. Shah, S.N.A.; Zheng, Y.; Li, H.; Lin, J.-M. Chemiluminescence character of ZnS quantum dots with bisulphite-hydrogen per-oxide system in acidic medium. *J. Phys. Chem. C* **2016**, *120*, 9308. [[CrossRef](#)]
24. Novič, M.; Grgič, I.; Poje, M.; Hudnik, V. Iron-catalyzed oxidation of s(IV) species by oxygen in aqueous solution: Influence of pH on the redox cycling of iron. *Atmos. Environ.* **1996**, *30*, 4191–4196. [[CrossRef](#)]
25. Brandt, C.; Van Eldik, R. Transition metal-catalyzed oxidation of sulfur (IV) oxides. Atmospheric-relevant processes and mechanisms. *Chem. Rev.* **1995**, *95*, 119. [[CrossRef](#)]
26. Lente, G.; Fábrián, I. Kinetics and mechanism of the oxidation of sulfur(iv) by iron(iii) at metal ion excess. *J. Chem. Soc. Dalton Trans.* **2002**, *5*, 778–784. [[CrossRef](#)]
27. Maaß, F.; Elias, H.; Wannowius, K.J. Kinetics of the oxidation of hydrogen sulfite by hydrogen peroxide in aqueous solution: Ionic strength effects and temperature dependence. *Atmos. Environ.* **1999**, *33*, 4413–4419. [[CrossRef](#)]
28. Shi, M.; Ding, J.; Liu, X.; Zhong, Q. Mechanisms of sulfite oxidation in sulfite-nitrite mixed solutions. *Atmos. Pollut. Res.* **2019**, *10*, 412–417. [[CrossRef](#)]
29. Lin, Z.; Chen, H.; Lin, J.-M. Peroxide induced ultra-weak chemiluminescence and its application in analytical chemistry. *Analyst* **2013**, *138*, 5182–5193. [[CrossRef](#)]
30. Li, R.; Kameda, T.; Toriba, A.; Hayakawa, K.; Lin, J.-M. Determination of benzo [a] pyrene-7, 10-quinone in airborne particulates by using a chemiluminescence reaction of hydrogen peroxide and hydrosulfite. *Anal. Chem.* **2012**, *84*, 3215. [[CrossRef](#)]
31. Xue, W.; Lin, Z.; Chen, H.; Lu, C.; Lin, J.-M. Enhancement of Ultraweak Chemiluminescence from Reaction of Hydrogen Peroxide and Bisulfite by Water-Soluble Carbon Nanodots. *J. Phys. Chem. C* **2011**, *115*, 21707–21714. [[CrossRef](#)]
32. Han, C.; Yuan, X.; Shen, Z.; Xiao, Y.; Wang, X.; Khan, M.; Liu, S.; Li, W.; Hu, Q.; Wu, W. A paper-based lateral flow sensor for the detection of thrombin and its inhibitors. *Anal. Chim. Acta* **2022**, *1205*, 339756. [[CrossRef](#)]
33. Timofeeva, I.I.; Vakh, C.S.; Bulatov, A.V.; Worsfold, P.J. Flow analysis with chemiluminescence detection: Recent advances and applications. *Talanta* **2018**, *179*, 246–270. [[CrossRef](#)]
34. Li, X.; Li, J.; Tang, J.; Kang, J.; Zhang, Y. Study of influence of metal ions on CdTe/ $\text{H}_2\text{O}_2$  chemiluminescence. *J. Lumin.* **2008**, *128*, 1229–1234. [[CrossRef](#)]
35. Zhang, C.; Jin, J.; Liu, K.; Ma, X.; Zhang, X. Carbon dots-peroxyoxalate micelle as a highly luminous chemiluminescence system under physiological conditions. *Chin. Chem. Lett.* **2021**, *32*, 3931–3935. [[CrossRef](#)]
36. Shah, S.A.; Hu, K.-J.; Naveed, M.; Shah, S.N.A.; Hu, S.; Lu, S.; Song, F. Synthesis of Au doped Ag nanoclusters and the doping effect of Au atoms on their physical and optical properties. *Mater. Res. Express* **2019**, *7*, 016506. [[CrossRef](#)]
37. Yu, X.; Wang, Q.; Liu, X.; Luo, X. A sensitive chemiluminescence method for the determination of cysteine based on silver nanoclusters. *Microchim. Acta* **2012**, *179*, 323–328. [[CrossRef](#)]
38. Fu, L.; Zhang, B.; Gao, X.; Dong, S.; Wang, D.; Zou, G. A General Route for Chemiluminescence of n-Type Au Nanocrystals. *Anal. Chem.* **2022**, *94*, 8811–8817. [[CrossRef](#)]
39. Wang, R.; Yue, N.; Fan, A. Nanomaterial-enhanced chemiluminescence reactions and their applications. *Analyst* **2020**, *145*, 7488–7510. [[CrossRef](#)]
40. Su, Y.; Xie, Y.; Hou, X.; Lv, Y. Recent Advances in Analytical Applications of Nanomaterials in Liquid-Phase Chemiluminescence. *Appl. Spectrosc. Rev.* **2013**, *49*, 201–232. [[CrossRef](#)]
41. Poznyak, S.K.; Talapin, D.V.; Shevchenko, E.V.; Weller, H. Quantum Dot Chemiluminescence. *Nano Lett.* **2004**, *4*, 693–698. [[CrossRef](#)]
42. Giokas, D.L.; Vlessidis, A.G.; Tsogas, G.Z.; Evmiridis, N.P. Nanoparticle-assisted chemiluminescence and its applications in analytical chemistry. *TrAC Trends Anal. Chem.* **2010**, *29*, 1113–1126. [[CrossRef](#)]

43. Adcock, J.L.; Barnett, N.W.; Barrow, C.J.; Francis, P.S. Advances in the use of acidic potassium permanganate as a chemiluminescence reagent: A review. *Anal. Chim. Acta* **2014**, *807*, 9. [[CrossRef](#)] [[PubMed](#)]
44. Shah, S.N.A.; Khan, M.; Rehman, Z.U. A prolegomena of periodate and peroxide chemiluminescence. *TrAC Trends Anal. Chem.* **2019**, *122*, 115722. [[CrossRef](#)]
45. Shah, S.N.A.; Li, H.; Lin, J.-M. Enhancement of periodate-hydrogen peroxide chemiluminescence by nitrogen doped carbon dots and its application for the determination of pyrogallol and gallic acid. *Talanta* **2016**, *153*, 23–30. [[CrossRef](#)] [[PubMed](#)]
46. Zheng, Y.; Zhang, D.; Shah, S.N.A.; Li, H.; Lin, J.-M. Ultra-weak chemiluminescence enhanced by facilely synthesized nitro-gen-rich quantum dots through chemiluminescence resonance energy transfer and electron hole injection. *Chem. Commun.* **2017**, *53*, 5657. [[CrossRef](#)] [[PubMed](#)]
47. Shah, S.N.A.; Dou, X.; Khan, M.; Uchiyama, K.; Lin, J.-M. N-doped carbon dots/H<sub>2</sub>O<sub>2</sub> chemiluminescence system for selective detection of Fe<sup>2+</sup> ion in environmental samples. *Talanta* **2018**, *196*, 370–375. [[CrossRef](#)]
48. Shah, S.N.A.; Lin, L.; Zheng, Y.; Zhang, D.; Lin, J.-M. Redox cycling of iron by carbon dot enhanced chemiluminescence: Mechanism of electron-hole induction in carbon dot. *Phys. Chem. Chem. Phys.* **2017**, *19*, 21604–21611. [[CrossRef](#)] [[PubMed](#)]
49. Lin, Z.; Xue, W.; Chen, H.; Lin, J.-M. Peroxynitrous-Acid-Induced Chemiluminescence of Fluorescent Carbon Dots for Nitrite Sensing. *Anal. Chem.* **2011**, *83*, 8245–8251. [[CrossRef](#)] [[PubMed](#)]
50. Shah, S.N.A.; Lin, J.-M. Recent advances in chemiluminescence based on carbonaceous dots. *Adv. Colloid Interface Sci.* **2017**, *241*, 24–36. [[CrossRef](#)]
51. Shah, S.N.A.; Shah, A.H.; Dou, X.; Khan, M.; Lin, L.; Lin, J.-M. Radical-Triggered Chemiluminescence of Phenanthroline Derivatives: An Insight into Radical-Aromatic Interaction. *ACS Omega* **2019**, *4*, 15004. [[CrossRef](#)]
52. Zhao, J.; Song, Q.; He, Q.; Dionysiou, D.D.; Wu, F.; Feng, Y.; Zhang, X. Fabrication of Bi<sub>1.81</sub>MnNbO<sub>6.72</sub>/sulfite system for efficient degradation of chlortetracycline. *Chemosphere* **2021**, *268*, 129269. [[CrossRef](#)]
53. McArdle, J.V.; Hoffmann, M.R. Kinetics and mechanism of the oxidation of aquated sulfur dioxide by hydrogen peroxide at low pH. *J. Phys. Chem.* **1983**, *87*, 5425–5429. [[CrossRef](#)]
54. Li, R.; Chen, H.; Li, Y.; Lu, C.; Lin, J.-M. Enhancing Effect of Alcoholic Solvent on Hydrosulfite-Hydrogen Peroxide Chemiluminescence System. *J. Phys. Chem. A* **2012**, *116*, 2192. [[CrossRef](#)] [[PubMed](#)]
55. Huie, R.E.; Neta, P. Rate constants for some oxidations of S(IV) by radicals in aqueous solutions. *Atmos. Environ. (1967)* **1987**, *21*, 1743–1747. [[CrossRef](#)]
56. Li, Q.; He, Y. An ultrasensitive chemiluminescence sensor for sub-nanomolar detection of manganese(II) ions in mineral water using modified gold nanoparticles. *Sens. Actuators B Chem.* **2017**, *243*, 454–459. [[CrossRef](#)]
57. Chen, H.; Shah, S.N.A.; Lin, J.-M. *Ultra-Weak Chemiluminescence from the Decomposition of Peroxymonocarbonate*; Springer: Berlin/Heidelberg, Germany, 2022; p. 17. [[CrossRef](#)]
58. Dou, X.; Zhang, Q.; Shah, S.N.A.; Khan, M.; Uchiyama, K.; Lin, J.-M. MoS<sub>2</sub>-quantum dot triggered reactive oxygen species generation and depletion: Responsible for enhanced chemiluminescence. *Chem. Sci.* **2018**, *10*, 497–500. [[CrossRef](#)] [[PubMed](#)]
59. Zhang, D.; Zheng, Y.; Dou, X.; Shah, S.N.A.; Lin, J.-M. Gas-phase chemiluminescence of reactive negative ions evolved through corona discharge in air and O<sub>2</sub> atmospheres. *RSC Adv.* **2017**, *7*, 15926–15930. [[CrossRef](#)]
60. Zhang, D.; Zheng, Y.; Dou, X.; Lin, H.; Shah, S.N.A.; Lin, J.-M. Heterogeneous Chemiluminescence from Gas-Solid Phase Interactions of Ozone with Alcohols, Phenols, and Saccharides. *Langmuir* **2017**, *33*, 3666. [[CrossRef](#)]
61. Li, J.; Li, Q.; Lu, C.; Zhao, L.; Lin, J.-M. Fluorosurfactant-capped gold nanoparticles-enhanced chemiluminescence from hydrogen peroxide-hydroxide and hydrogen peroxide-bicarbonate in presence of cobalt (II). *Spectrochim. Acta A Mol. Biomole. Spectrosc.* **2011**, *78*, 700. [[CrossRef](#)]
62. Chen, H.; Li, H.; Lin, J.-M. Determination of ammonia in water based on chemiluminescence resonance energy transfer between peroxymonocarbonate and branched NaYF<sub>4</sub>: Yb<sup>3+</sup>/Er<sup>3+</sup> nanoparticles. *Anal. Chem.* **2012**, *84*, 8871. [[CrossRef](#)]
63. Huang, X.; Ren, J. Nanomaterial-based chemiluminescence resonance energy transfer: A strategy to develop new analytical methods. *TrAC Trends Anal. Chem.* **2012**, *40*, 77–89. [[CrossRef](#)]
64. Freeman, R.; Liu, X.; Willner, I. Chemiluminescent and Chemiluminescence Resonance Energy Transfer (CRET) Detection of DNA, Metal Ions, and Aptamer-Substrate Complexes Using Hemin/G-Quadruplexes and CdSe/ZnS Quantum Dots. *J. Am. Chem. Soc.* **2011**, *133*, 11597–11604. [[CrossRef](#)]
65. Amjadi, M.; Hallaj, T.; Mirbirang, F. A chemiluminescence reaction consisting of manganese(IV), sodium sulfite, and sulfur- and nitrogen-doped carbon quantum dots, and its application for the determination of oxytetracycline. *Microchim. Acta* **2020**, *187*, 191. [[CrossRef](#)] [[PubMed](#)]
66. Li, L.; Lai, X.; Xu, X.; Li, J.; Yuan, P.; Feng, J.; Wei, L.; Cheng, X. Determination of bromate via the chemiluminescence generated in the sulfite and carbon quantum dot system. *Microchim. Acta* **2018**, *185*, 136. [[CrossRef](#)] [[PubMed](#)]
67. Zhang, J.; Han, S. Strong Enhancement of the Chemiluminescence of Hydrogen Sulfite-Oxidant Systems in the Presence of N,S-Doped Graphene Quantum Dots, and Its Application to the Determination of Folic Acid in Spinach and Kiwifruit Samples. *Food Anal. Methods* **2019**, *12*, 869–876. [[CrossRef](#)]
68. Li, D.; Nie, F.; Tang, T.; Tian, K. Determination of ferric ion via its effect on the enhancement of the chemiluminescence of the permanganate-sulfite system by nitrogen-doped graphene quantum dots. *Microchim. Acta* **2018**, *185*, 431. [[CrossRef](#)] [[PubMed](#)]
69. Liu, H.; Su, Y.; Deng, D.; Song, H.; Lv, Y. Chemiluminescence of Oleic Acid Capped Black Phosphorus Quantum Dots for Highly Selective Detection of Sulfite in PM<sub>2.5</sub>. *Anal. Chem.* **2019**, *91*, 9174–9180. [[CrossRef](#)] [[PubMed](#)]

70. Yu, X.; Bao, J. Determination of norfloxacin using gold nanoparticles catalyzed cerium (IV)–sodium sulfite chemiluminescence. *J. Lumin.* **2009**, *129*, 973. [[CrossRef](#)]
71. Yu, X.; Jiang, Z.; Wang, Q.; Guo, Y. Silver nanoparticle-based chemiluminescence enhancement for the determination of norfloxacin. *Microchim. Acta* **2010**, *171*, 17–22. [[CrossRef](#)]
72. Kamruzzaman, M.; Alam, A.-M.; Kim, K.M.; Lee, S.H.; Kim, Y.H.; Kim, S.H. Silver Nanoparticle-Enhanced Chemiluminescence Method for Determining Naproxen Based on Europium(III)-Sensitized Ce(IV)-Na<sub>2</sub>S<sub>2</sub>O<sub>4</sub> Reaction. *J. Fluoresc.* **2012**, *22*, 883–890. [[CrossRef](#)]
73. Kouhestany, R.H.; Azizi, S.N.; Shakeri, P.; Rahmani, S. Sensitive Determination of Cetirizine Using CdS Quantum dots as Oxidase Mimic-mediated Chemiluminescence of Sulfite. *Int. Curr. Pharm. J.* **2016**, *5*, 59–62. [[CrossRef](#)]
74. Sun, C.; Liu, B.; Li, J. Sensitized chemiluminescence of CdTe quantum-dots on Ce(IV)-sulfite and its analytical applications. *Talanta* **2008**, *75*, 447–454. [[CrossRef](#)]
75. Chen, H.; Xue, W.; Lu, C.; Li, H.-f.; Zheng, Y.; Lin, J.-M. Plasmonic luminescent core–shell nanocomposites-enhanced chemiluminescence arising from the decomposition of peroxomonosulfite. *Spectrochim. Acta A Mole. Biomole. Spectrosc.* **2013**, *116*, 355. [[CrossRef](#)]
76. Sun, T.; Su, Y.; Liu, H.; Song, H.; Lv, Y. Efficient generation of sulfate radicals in Fe(II)/S(IV) system induced by WS<sub>2</sub> nanosheets and examined by its intrinsic chemiluminescence. *Chem. Commun.* **2020**, *56*, 6993. [[CrossRef](#)]
77. Li, Q.; Sun, M.; Su, Y.; Zhang, K.; Lv, Y. Efficient chemiluminescence resonance energy transfer on the interface of europium doped ceria for sulfite detection in PM<sub>2.5</sub>. *Sens. Actuators B Chem.* **2021**, *339*, 129876. [[CrossRef](#)]
78. Zhang, X.; He, S.; Chen, Z.; Huang, Y. CoFe<sub>2</sub>O<sub>4</sub> Nanoparticles as Oxidase Mimic-Mediated Chemiluminescence of Aqueous Luminol for Sulfite in White Wines. *J. Agric. Food Chem.* **2013**, *61*, 840–847. [[CrossRef](#)] [[PubMed](#)]
79. Zhang, Y.; Zhou, J.; Li, C.; Guo, S.; Wang, G. Reaction Kinetics and Mechanism of Iron(II)-Induced Catalytic Oxidation of Sulfur(IV) during Wet Desulfurization. *Ind. Eng. Chem. Res.* **2012**, *51*, 1158–1165. [[CrossRef](#)]
80. Lian, N.; Tang, J.H.; He, X.H. Determination of gatifloxacin in drug formulations, human urine, and serum samples using energy transfer chemiluminescence coupled with flow-injection analysis. *J. Anal. Chem.* **2014**, *69*, 276–282. [[CrossRef](#)]
81. Yi, L.; Zhao, H.; Chen, S.; Jin, L.; Zheng, D.; Wu, Z. Flow-injection analysis of two fluoroquinolones by the sensitizing effect of terbium(III) on chemiluminescence of the potassium permanganate–sodium sulfite system. *Talanta* **2003**, *61*, 403–409. [[CrossRef](#)]
82. Zhang, W.; Liu, H.; Zhang, F.; Wang, Y.-L.; Song, B.; Zhang, R.; Yuan, J. Development of a ruthenium (II) complex-based luminescence probe for detection of hydrogen sulfite in food samples. *Microchem. J.* **2018**, *141*, 181. [[CrossRef](#)]
83. Cao, W.; Gong, P.; Liu, W.; Zhuang, M.; Yang, J. A sensitive flow injection chemiluminescence method for the determination of progesterone. *Drug Test. Anal.* **2011**, *5*, 242–246. [[CrossRef](#)]
84. Yan, Z.; Zhang, Z.; Yu, Y.; Liu, Z.; Chen, J. Chemiluminescence determination of potassium bromate in flour based on flow injection analysis. *Food Chem.* **2016**, *190*, 20–24. [[CrossRef](#)] [[PubMed](#)]
85. Meng, H.; Wu, F.; He, Z. Chemiluminescence determination of sulfite in sugar and sulfur dioxide in air using Tris (2,2'-bipyridyl) ruthenium (II)-permanganate system. *Talanta* **1999**, *48*, 571. [[CrossRef](#)] [[PubMed](#)]
86. Wu, F.; He, Z.; Meng, H.; Zeng, Y. Determination of sulfite in sugar and sulfur dioxide in air by chemiluminescence using the Ru(bipy)<sub>3</sub><sup>2+</sup>–KBrO<sub>3</sub> system. *Analyst* **1998**, *123*, 2109–2112. [[CrossRef](#)]
87. Bonifácio, R.L.; Coichev, N. Chemiluminescent determination of sulfite traces based on the induced oxidation of Ni(II)/tetraglycine complex by oxygen in the presence of luminol: Mechanistic considerations. *Anal. Chim. Acta* **2004**, *517*, 125. [[CrossRef](#)]
88. Huang, Y.; Zhang, C.; Zhang, X.; Zhang, Z. Chemiluminescence of sulfite based on auto-oxidation sensitized by rhodamine 6G. *Anal. Chim. Acta* **1999**, *391*, 95–100. [[CrossRef](#)]
89. He, D.; Zhang, Z.; Huang, Y. Chemiluminescence Microflow Injection Analysis System on a Chip for the Determination of Sulfite in Food. *Anal. Lett.* **2005**, *38*, 563–571. [[CrossRef](#)]
90. Huang, Y.; Zhang, C.; Zhang, X.; Zhang, Z. A Sensitive Chemiluminescence Flow System for the Determination of Sulfite. *Anal. Lett.* **1999**, *32*, 1211–1224. [[CrossRef](#)]
91. Zhang, S.; Zhuang, Y.; Ju, H. Flow-Injection Chemiluminescence Determination of Papaverine Using Cerium(IV)-Sulfite System. *Anal. Lett.* **2004**, *37*, 143–155. [[CrossRef](#)]
92. Mokhtari, A.; Aagha, M.H.M. Chemiluminescence System of Permanganate-Sulfite for Simple Determination of Zolpidem. *Eurasian J. Anal. Chem.* **2017**, *12*, 61–74. [[CrossRef](#)]
93. Navarro, M.V.; Payán, M.R.; López, M.A.B.; Fernández-Torres, R.; Mochón, M.C. Rapid flow injection method for the determination of sulfite in wine using the permanganate–luminol luminescence system. *Talanta* **2010**, *82*, 2003. [[CrossRef](#)]
94. Al-Tamrah, S.A.; Townshend, A.; Wheatley, A.R. Flow injection chemiluminescence determination of sulphite. *Analyst* **1987**, *112*, 883–886. [[CrossRef](#)]
95. Qin, W.; Zhang, Z.; Zhang, C. Reagentless chemiluminescence flow sensor for sulfite. *Anal. Chim. Acta* **1998**, *361*, 201–203. [[CrossRef](#)]
96. Qin, W.; Zhang, Z.-J.; Zhang, C.-J. Chemiluminescence flow system for the determination of sulfite. *Anal. Bioanal. Chem.* **1998**, *361*, 824–826. [[CrossRef](#)]
97. Yamada, M.; Nakada, T.; Suzuki, S. The determination of sulfite in a flow injection system with chemiluminescence detection. *Anal. Chim. Acta* **1983**, *147*, 401–404. [[CrossRef](#)]

98. Li, Q.; Yan, S.; Song, H.; Su, Y.; Sun, M.; Lv, Y. A simple and stable chemiluminescence resonance energy transfer system based on Ce(IV)-MOFs for detection of sulfite. *Sens. Actuators B Chem.* **2023**, *376*, 132990. [[CrossRef](#)]
99. Guo-Fang, Z.; Hong-Yuan, C. Studies of micelle and trace non-polar organic solvent on a new chemiluminescence system and its application to flow injection analysis. *Anal. Chim. Acta* **2000**, *409*, 75–81.
100. Frigerio, C.; Ribeiro, D.S.; Rodrigues, S.S.M.; Abreu, V.L.; Barbosa, J.A.; Prior, J.A.; Marques, K.L.; Santos, J.L. Application of quantum dots as analytical tools in automated chemical analysis: A review. *Anal. Chim. Acta* **2012**, *735*, 9–22. [[CrossRef](#)]
101. Liu, Y.; Cao, M.; Huang, Z.; Yu, C.; Yang, N.; Wu, Q.; Shi, L.; Duan, W.; Zhu, Y.; Wei, J.; et al. Ultrasensitive detection of IgE levels based on magnetic nanocapturer linked immunosensor assay for early diagnosis of cancer. *Chin. Chem. Lett.* **2021**, *33*, 1855–1860. [[CrossRef](#)]
102. Zhao, H.; Su, E.; Huang, L.; Zai, Y.; Liu, Y.; Chen, Z.; Li, S.; Jin, L.; Deng, Y.; He, N. Washing-free chemiluminescence immunoassay for rapid detection of cardiac troponin I in whole blood samples. *Chin. Chem. Lett.* **2022**, *33*, 743. [[CrossRef](#)]
103. Huang, L.; Su, E.; Liu, Y.; He, N.; Deng, Y.; Jin, L.; Chen, Z.; Li, S. A microfluidic device for accurate detection of hs-cTnI. *Chin. Chem. Lett.* **2021**, *32*, 1555. [[CrossRef](#)]
104. Li, N.; Zhang, W.; Lin, H.; Lin, J.-M. Di-4-ANEPPDHQ probes the response of lipid packing to the membrane tension change in living cells. *Chin. Chem. Lett.* **2021**, *33*, 1377–1380. [[CrossRef](#)]
105. Pan, Y.; Deng, F.-F.; Fang, Z.; Chen, H.-J.; Long, Z.; Hou, X.-D. Integration of cryogenic trap to gas chromatography-sulfur chemiluminescent detection for online analysis of hydrogen gas for volatile sulfur compounds. *Chin. Chem. Lett.* **2021**, *32*, 3440–3445. [[CrossRef](#)]
106. Wang, Z.; Gao, H.; Liu, P.; Wu, X.; Li, Q.; Xu, J.-J.; Hua, D. Visualized uranium rapid monitoring system based on self-enhanced electrochemiluminescence-imaging of amidoxime functionalized polymer nanoparticles. *Chin. Chem. Lett.* **2022**, *33*, 3456–3460. [[CrossRef](#)]
107. Ting, L.; Xuyang, C.; Kai, W.; Zhigang, H. Small-Molecule Fluorescent Probe for Detection of Sulfite. *Pharmaceuticals* **2022**, *15*, 1326.
108. Pundir, C.S.; Rawal, R. Determination of sulfite with emphasis on biosensing methods: A review. *Anal. Bioanal. Chem.* **2013**, *405*, 3049–3062. [[CrossRef](#)] [[PubMed](#)]
109. Qin, W.; Su, L.; Yang, C.; Ma, Y.; Zhang, H.; Chen, X. Colorimetric Detection of Sulfite in Foods by a TMB-O<sub>2</sub>-Co<sub>3</sub>O<sub>4</sub> Nanoparticles Detection System. *J. Agric. Food Chem.* **2014**, *62*, 5827. [[CrossRef](#)] [[PubMed](#)]
110. Xing, G.; Zhang, W.; Li, N.; Pu, Q.; Lin, J.-M. Recent progress on microfluidic biosensors for rapid detection of pathogenic bacteria. *Chin. Chem. Lett.* **2022**, *33*, 1743–1751. [[CrossRef](#)]
111. Gul, E.; Rahman, G.; Wu, Y.; Bokhari, T.H.; Rahman, A.U.; Zafar, A.; Rana, Z.; Shah, A.; Hussain, S.; Maaz, K.; et al. An amphiphilic polyoxometalate-CNT nanohybrid as a highly efficient enzyme-free electrocatalyst for H<sub>2</sub>O<sub>2</sub> sensing. *New J. Chem.* **2022**, *46*, 16280. [[CrossRef](#)]
112. Chen, H.; Lin, L.; Li, H.; Li, J.; Lin, J.-M. Aggregation-Induced Structure Transition of Protein-Stabilized Zinc/Copper Nanoclusters for Amplified Chemiluminescence. *ACS Nano* **2015**, *9*, 2173–2183. [[CrossRef](#)]
113. Al-Mugahiry, B.; Al-Lawati, H.A.J. Recent analytical advancements in microfluidics using chemiluminescence detection systems for food analysis. *TrAC Trends Anal. Chem.* **2020**, *124*, 115802. [[CrossRef](#)]
114. Roda, A.; Guardigli, M.; Pasini, P.; Mirasoli, M. Bioluminescence and chemiluminescence in drug screening. *Anal. Bioanal. Chem.* **2003**, *377*, 826–833. [[CrossRef](#)]

**Disclaimer/Publisher’s Note:** The statements, opinions and data contained in all publications are solely those of the individual author(s) and contributor(s) and not of MDPI and/or the editor(s). MDPI and/or the editor(s) disclaim responsibility for any injury to people or property resulting from any ideas, methods, instructions or products referred to in the content.